PHYSICAL REVIEW
LETTERS

VOLUME 6 JANUARY 1, 1961 NUMBER 1

NUCLEAR PARAMAGNETIC SUSCEPTIBILITY OF THE POSSIBLE LOW-TEMPERATURE PHASE OF LIQUID He^3†

L. H. Nosanow and R. Vasudevan
University of California, La Jolla, California
(Received November 21, 1960)

Recently it has been suggested[1-3] that liquid He^3 will undergo a phase transition to a highly correlated phase at a temperature of approximately 0.06 degree. This suggestion is based upon a model of the BCS[4] type which is modified to take into account the attraction of two He^3 atoms in relative d states near the Fermi surface. This model predicts a second order phase transition, even though it requires the existence of an arbitrary direction in the low-temperature phase. A convenient experiment to detect this transition is a measurement of the magnetic susceptibility. Therefore, we have calculated the behavior of the system in the presence of a uniform magnetic field using the model of BSAM. We wish to emphasize that this model can not be expected to yield detailed quantitative results. However, if the attraction near the Fermi surface can cause a transition to a highly correlated state, then it is reasonable to suppose that this model will give the gross features of the low-temperature phase correctly.

We have made the calculation for arbitrary fields using the method of Bogoliubov et al.[5] It is possible to do this because the term containing the field remains diagonal under the Bogoliubov transformation. It turns out that the angle between the field and the arbitrary direction does not enter anywhere in the result. For small fields, our result, which takes into account the interaction in relative d states, is the appropriate generalization of the result previously obtained by Yosida[6] for the spherically symmetric case. We also find for quite general interactions that at each temperature below the critical temperature, there exists a critical magnetic field above which the low-temperature phase can not exist. At the critical field the system undergoes a second order phase transition.

In our calculation we shall use the notation of BZT unless otherwise specified. We take as our Hamiltonian

$$H = H_{BZT} - \kappa \sum_k (a_{k+}^{\dagger} a_{k+} - a_{-k-}^{\dagger} a_{-k-}), \qquad (1)$$

where κ is the magnetic field multiplied by the appropriate magneton for He^3. Since the second term in (1) remains diagonal under the Bogoliubov transformation, it is straightforward to apply the method of BZT. The only differences are that we need to allow for complex parameters in the Bogoliubov transformation, and that the final evaluation of traces is different due to the change in energy of each state due to the field. The result for the thermodynamic potential is

$$\psi = \sum_k \left\{ E(k) - \lambda - \Omega(k) + \frac{|c(k)|^2}{2\Omega(k)} t\left(\frac{\Omega(k)}{\theta}, \frac{\kappa}{\theta}\right) - \theta \ln\left\{\left[1 + \exp\left(-\frac{[\Omega(k)+\kappa]}{\theta}\right)\right]\left[1 + \exp\left(-\frac{[\Omega(k)-\kappa]}{\theta}\right)\right]\right\}\right\}, \qquad (2)$$

where

$$\Omega(k)=\pm\{[E(k)-\lambda]^2+|c(k)|^2\}^{1/2}, \quad (3)$$

the + sign being taken for $E(k)>\lambda$ and the - sign for $E(k)<\lambda$,

$$t(x,y)=\sinh x/(\cosh x+\cosh y), \quad (4)$$

and the auxiliary parameter $c(k)$ (which is the energy gap in the spherically symmetric case) is given by

$$c(k)=\frac{1}{V}\sum_{k'}J(k,k')\frac{c(k')}{2\Omega(k')}t(\Omega(k')/\theta,\kappa/\theta). \quad (5)$$

Equation (5) shows that $c(k)$ is nonvanishing only for values of k for which $J(k,k')$ is nonvanishing. It always possesses the trivial solution $c(k)=0$, in which case (2) reduces to the well-known expression for ψ for an ideal Fermi gas in the presence of a uniform magnetic field. From (4) we see that $t(x,0)=\tanh\frac{1}{2}x$, so that (2) reduces to the BZT result in the absence of the field. In addition

$$\lim_{x\to 0}t(x,y)=0 \quad \text{and} \quad \lim_{y\to\infty}t(x,y)=0, \quad (6)$$

so that (5) can only have solutions for sufficiently low temperatures and sufficiently low fields. Thus we see quite generally that there is a critical magnetic field. This result is not of any practical importance since fields of the order of 10^6 gauss would be needed to observe the critical field even near the critical temperature. Finally, from the form of $t(x,y)$ and ψ, we see that the angle between the field and the arbitrary direction does not enter into the result. Hence for simplicity we may take the field along the arbitrary direction.

To make a more detailed analysis, we take the interaction to be

$$\frac{1}{V}J(k,k')=V_l(2l+1)P_l(k,k'), \quad (7)$$

for $E(k)$ and $E(k')$ within the energy shell of width 2ω centered about the Fermi surface, and make the ansatz

$$c(k)=\epsilon_{lm}Y_l^m(k,k_0). \quad (8)$$

Both (7) and (8) are the same as in BSAM. After using (7) and (8) and the addition theorem for Legendre polynomials, (5) becomes

$$1=4\pi V_l\sum_k\frac{|Y_l^m|^2}{2\Omega(k)}t(\Omega(k)/\theta,\kappa/\theta), \quad (9)$$

which shows that ϵ_{lm} is a function of both θ and κ in general. Near the transition at a point θ_1, κ_1 where ϵ_{lm} is small, it is easy to show that

$$\epsilon_{lm}{}^2\approx\text{constant}(\theta-\theta_1)+\text{constant}(\kappa-\kappa_1), \quad (10)$$

from which it follows that the system undergoes a second order transition at the critical temperature or the critical field.

We may now compute the magnetic susceptibility χ by differentiating ψ with respect to the field. It is necessary to include the dependence of ϵ_{lm} on the field. One finds

$$\chi=\frac{1}{\kappa}\sum_k\frac{\sinh(\kappa/\theta)}{\cosh(\kappa/\theta)+\cosh[\Omega(k)/\theta]}, \quad (11)$$

where $\Omega(k)$ reduces to $E(k)$ outside the spherical shell of width 2ω centered on the Fermi surface. For small fields (up to the order of 10^5 gauss), (11) reduces to

$$\frac{\chi}{\chi_N}=\frac{1}{2\theta}\int_0^\omega dx\int\frac{d\Omega}{4\pi}\operatorname{sech}^2\left[\frac{1}{2\theta}\{x^2+[\epsilon_{lm}(0)]^2|Y_l^m|^2\}^{1/2}\right], \quad (12)$$

where χ_N is the susceptibility of the normal system, and $\epsilon_{lm}(0)$ is ϵ_{lm} for zero field. Clearly (12) reduces to Yosida's result in the spherically symmetric case. Numerical integration of (12) for the case $l=2$, $m=2$ yields the curve pictured in Fig. 1. We have chosen this case since it is one of the choices of l and m which

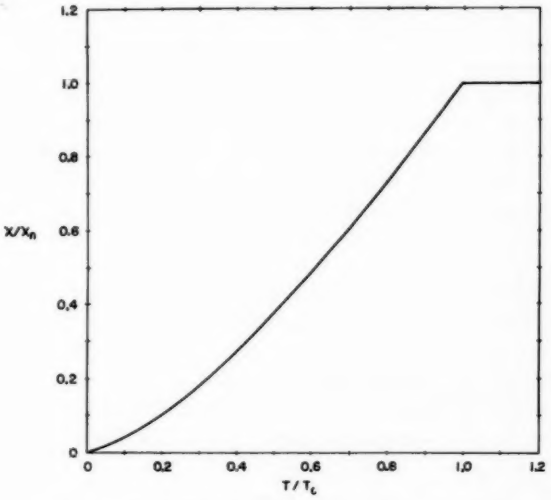

FIG. 1. Temperature dependence of the paramagnetic susceptibility of He^3.

minimizes the free energy.[7]

Since the magnetic susceptibility prediction of the BCS theory does not agree with experiment for very low temperatures, the above calculation can only be considered as valid near the critical temperature. The main point is that an attraction in He^3 in relative d states predicts a rather sharp drop in the susceptibility at the critical temperature. This will not be true if it were an attraction in relative s or f states because in this case the Cooper pairs will be formed from particles with parallel spins, and therefore the susceptibility will be the same as that of the normal fluid at all temperatures.

The magnetic susceptibility has been measured by Wheatley et al.,[8] who find no sharp change down to 0.035 degree. Thus the present experimental evidence does not indicate the existence of a highly correlated low-temperature phase of He^3 above 0.035 degree.

We wish to thank Professor Keith Brueckner for suggesting this problem to us and for stimulating discussions.

†This work was supported by the U. S. Atomic Energy Commission.

[1]K. A. Brueckner, T. Soda, P. W. Anderson, and P. Morel, Phys. Rev. 118, 1442 (1960). Hereafter referred to as BSAM.

[2]V. J. Emery and A. M. Sessler, Phys. Rev. 119, 43 (1960).

[3]L. P. Pitaevskii, J. Exptl. Theoret. Phys. (U.S.S.R.) 37, 1794 (1959) [translation: Soviet Phys. - JETP 10, 1267 (1960)].

[4]J. Bardeen, L. N. Cooper, and J. R. Schrieffer, Phys. Rev. 108, 1175 (1957).

[5]N. N. Bogoliubov, D. N. Zubarev, and Yu. A. Tserkovnikov, Doklady Akad. Nauk S.S.S.R. 117, 788 (1957) [translation: Soviet Phys. Doklady 2, 535 (1957)]. See also N. N. Bogoliubov, V. V. Tolmachev, and D. V. Shirkov, A New Method in the Theory of Superconductivity (Consultants Bureau, Inc., New York, 1959), Sec. 8.1.

[6]Kei Yosida, Phys. Rev. 110, 769 (1958).

[7]T. Soda and R. Vasudevan (to be published).

[8]A. C. Anderson, H. R. Hart, Jr., and J. C. Wheatley, Phys. Rev. Letters 5, 133 (1960).

LIMITING VALUE OF DEBYE TEMPERATURE FOR SUPERCONDUCTING AND NORMAL INDIUM FROM LOW-TEMPERATURE ELASTIC CONSTANTS

B. S. Chandrasekhar and J. A. Rayne
Westinghouse Research Laboratories, Pittsburgh, Pennsylvania
(Received November 10, 1960)

A significant difference between the lattice heat capacity of indium in the superconducting and normal states has recently been reported.[1] Since only long-wavelength phonons are excited in a solid at low temperatures, one would therefore expect a corresponding difference in the elastic properties of indium in the two phases. This note gives the results of elastic constant measurements on superconducting and normal indium. These measurements form part of an extended study of the elastic properties of indium to be reported in detail later.

The elastic constants were measured, using the usual ultrasonic pulse technique,[2] on single crystals grown from 99.999% pure indium. By observing a distant echo on an expanded delayed sweep, any change in transit time could be measured to an accuracy of about 1 part in 2×10^4, i. e., a change in the associated elastic constant of about 1 part in 10^4 could be detected. At 1.4°K the change in transit time for every propagation mode was less than the above limit of detectability, when the samples were taken from the superconducting to normal state by applying a quenching field of 800 oersteds. Thus the difference between the values of any elastic constant of indium in the two phases is less than 1 part in 10^4. This result is consistent with the much smaller change in elastic constants on going from the superconducting to normal phase predicted thermodynamically. Such a change, of the order of 1 part in 10^6, has been observed in lead and tin.[3] Now it has been shown that in many metals,[4] and particularly tin,[5] there is excellent agreement between the lattice heat capacity computed from the elastic constants extrapolated to 0°K and that measured calorimetrically. It is therefore felt that the present results show that the difference in lattice heat capacity between normal and superconducting indium is less than 1 part in 6×10^3.

The values of the elastic constants of indium, extrapolated to 0°K, are $c_{11}=5.39$, $c_{12}=3.87$, $c_{13}=4.51$, $c_{33}=5.16$, $c_{44}=0.797$, and $c_{66}=1.68$,

all in units of 10^{11} dyne cm^{-2}. From these data, the limiting value of Debye temperature θ for indium was calculated numerically by the method described elsewhere.[5] The value obtained is

$$\theta = 111.3^\circ\text{K}, \qquad (1)$$

with an estimated uncertainty about one percent.

At sufficiently low temperatures, the heat capacity of superconducting indium can be expressed as

$$C_s = \alpha_s T^3 + C_q, \qquad (2)$$

where C_q is the nuclear quadrupole heat capacity. Thus a plot of $(C_S - C_q)/T$ versus T^2 should be a straight line through the origin. Such a plot obtained from the calorimetric data[1] is shown in Fig. 1. The straight line through the origin has been drawn to give a slope corresponding to the value of Debye temperature obtained above. A parallel line has been drawn through the normal state points. It can be seen that this latter line gives a good fit to the data below about 0.7°K; the corresponding value of the coefficient of the electronic heat capacity is $\gamma = 1.65$ millijoule mole^{-1} deg^{-2}. At low temperatures the calorimetric data in the superconducting state lie considerably below the computed line. The discrepancy is well outside the estimated uncertainty in the slope of the latter. The calorimetric data for $T > 0.7$°K doubtless include an electronic contribution. Bryant and Keesom[1] state that below this temperature the electronic term is negligible; even if this were not strictly correct, the discrepancy between the lattice heat capacity computed in the present work and that measured calorimetrically would only be greater. No reasonable explanation of this discrepancy can be advanced.

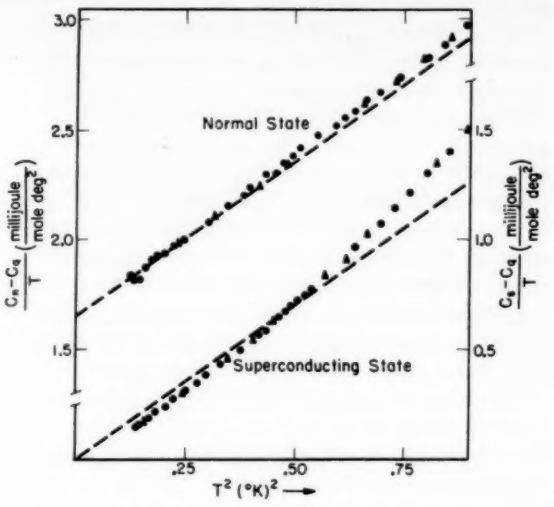

FIG. 1. A plot of $(C_n - C_q)/T$ and $(C_S - C_q)/T$ versus T^2, from reference 1. The broken straight lines are drawn with a slope corresponding to $\theta = 111.3$°K.

[1]C. A. Bryant and P. H. Keesom, Phys. Rev. Letters 4, 460 (1960).
[2]J. A. Rayne, Phys. Rev. 115, 63 (1959).
[3]W. P. Mason and H. E. Bommel, J. Acoust. Soc. Am. 28, 930 (1956); B. Welber and S. L. Quimby, Acta Met. 6, 351 (1958); D. F. Gibbons and C. A. Renton, Phys. Rev. 114, 1257 (1959).
[4]G. A. Alers and J. R. Neighbours, Revs. Modern Phys. 31, 675 (1959).
[5]J. A. Rayne and B. S. Chandrasekhar, Phys. Rev. 120, 1658 (1960).

RESOLVED HYPERFINE SPECTRA OF ELECTRON-SPIN PARAMAGNETIC RESONANCE IN IRRADIATED LiF†

Y. W. Kim,* R. Kaplan, and P. J. Bray
Department of Physics, Brown University, Providence, Rhode Island
(Received December 1, 1960)

Recently, Holton, Blum, and Slichter[1] reported on the resolved hyperfine spectra of the electron-spin paramagnetic resonance (ESPR) absorption of F centers in x-irradiated single crystals of LiF. Their spectra are nearly Gaussian in shape with a width (ΔH) of 85 ± 10 gauss from peak to center of the derivative of the ESPR absorption curve. The center of resonance (H_0) of each spectrum corresponds to $g = 2.0006 \pm 0.0006$. The resolved hyperfine lines, 35 in number, are uniformly spaced, the spacing being approximately 14 gauss when the magnetic field (H) is parallel to a [100] axis or a [111] axis of the sample. No variation of the spacing with orientations of the samples in the magnetic field was reported. Further, Holton et al.[1] measured, by means of electron-nuclear double resonance, the hyperfine coupling constants of the F-center

electron with nuclei up to and including the eighth shell of nuclei surrounding the F^- ion vacancy. The measured values of these constants agree approximately with values predicted by Gourary and Adrian.[2]

In the present Letter evidence will be presented supporting the view that the hyperfine structure observed in the ESPR spectra of irradiated LiF cannot be ascribed simply to the presence of F centers in the crystal. This evidence has been obtained from comprehensive investigations[3] of LiF single crystals obtained from the Harshaw Chemical Company and exposed at room temperature to 40-kv x rays, thermal neutrons, or γ rays over a large range of doses. A Varian Model V-4500 spectrometer was employed to obtain the ESPR spectra at either 300°K or 77°K. The hyperfine spectra obtained differ from those of Holton et al. with respect to shape, width, g value, and angular dependence.

Two distinct shapes of ESPR spectra were observed. One was Gaussian, and the other Lorentzian. The spectra of Gaussian shape were obtained from samples which were irradiated with x rays, γ rays, and neutrons, with doses up to 10^{18} *nvt*. These spectra gave values of $\Delta H = 60 \pm 6$ gauss and $g = 2.0027 \pm 0.0004$, regardless of the radiation dose. The concentration of electron spins responsible for the Gaussian resonance was found to be of the order of $10^{17}/\text{cm}^3$ for neutron doses of approximately 10^{14} *nvt*. It increased almost linearly for neutron doses up to about 10^{16} *nvt*, after which it asymptotically approached a constant value of the order of $10^{20}/\text{cm}^3$. In these samples it was found that the concentration of F centers estimated by means of optical absorption agreed, in order of magnitude, with the concentration of electron spins found for various neutron doses. By means of power saturation, this Gaussian resonance was found to be inhomogeneously broadened. Spectra of Lorentzian shape were obtained from some samples with neutron doses of approximately 10^{16} *nvt* or more. H_0 of these spectra corresponds to $g = 2.0023 \pm 0.0004$. The observed ΔH varied from sample to sample, with a maximum value of 35 ± 4 gauss, and appeared to decrease as neutron doses increased. In an earlier paper, the authors have associated the Lorentzian resonances with conduction electrons in Li metal grains formed in LiF.[4]

The anisotropy of the ESPR spectrum was investigated by rotating the sample about its [110] axis, which was held perpendicular to the direction of the magnetic field. In this case, the magnetic field sweeps over the (110) plane of the sample. The angle between the [001] axis and H direction is denoted by α.

All spectra, whether Gaussian or Lorentzian in shape, clearly exhibited partially resolved hyperfine lines of uniform spacing at $\alpha = 0°$, 55°, 72°, and 90°, while they were unresolved and "smooth" at $\alpha = 25°$ and 80°. For both shapes of spectra, the spacing of lines at $\alpha = 0°$, 55°, 72°, and 90° is approximately 14 gauss, 14 gauss, 7 gauss, and 12.5 gauss, respectively. The change of a resolved spectrum (or a smooth spectrum) into a smooth spectrum (or a resolved spectrum) as α increases from 0° to 90° takes place gradually. Figure 1 exhibits a resolved hyperfine spectrum of Gaussian shape with $\Delta H = 60 \pm 6$ gauss, which was observed near $\alpha = 72°$. The uniform spacing between lines is 7 gauss. Figure 2 shows a resolved hyperfine spectrum of Lorentzian shape with $\Delta H = 35 \pm 4$ gauss which was observed at $\alpha = 55°$. The resolved hyperfine lines are spaced 14 gauss apart. Table I lists the anistropy of line spacing, and the number of resolved hyperfine lines. It should be noted that, in spite of the anisotropy of line spacing, the envelopes of the resolved spectra of both shapes exhibited no noticeable dependence on α.

Some resonance curves of Gaussian shape were transformed into Lorentzian or other shapes by heat-treating the sample. A sample with 4.2×10^{16} *nvt* irradiation, and a sample with 5×10^{16} *nvt* irradiation, both of which yielded the Gaussian

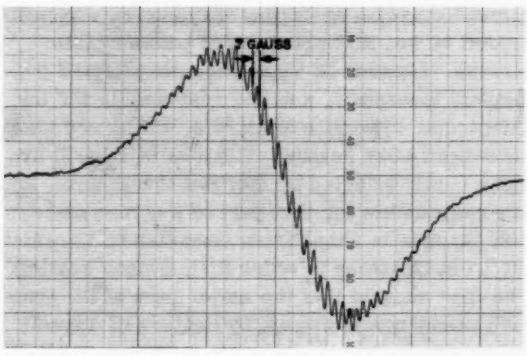

FIG. 1. Resolved hyperfine spectrum of Gaussian shape representing an ESPR absorption in an irradiated single crystal of LiF (neutron dose: 1.3×10^{15} *nvt*), when the angle of rotation, α, is near 72°. The center of resonance H_0 corresponds to $g = 2.0027 \pm 0.0004$, and the spacing between neighboring hyperfine lines is approximately 7 gauss.

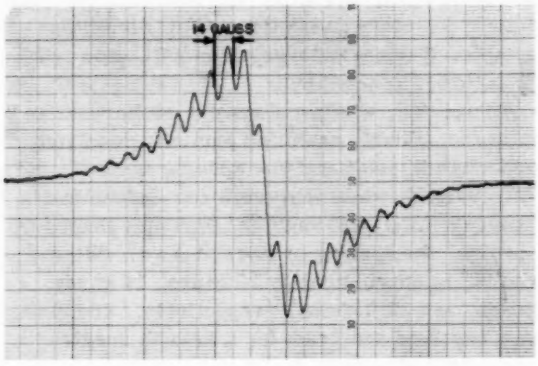

FIG. 2. Resolved hyperfine spectrum of Lorentzian shape representing an ESPR absorption in an irradiated single crystal of LiF (neutron dose: 9.9×10^{17} *nvt*), when the angle of rotation, α, is 55°. The center of resonance corresponds to $g = 2.0023 \pm 0.0004$, and the spacing between neighboring hyperfine lines is 14 gauss.

shape of ESPR spectrum, were heat treated for two hours at 250°C, followed by a rapid quenching to room temperature, and for one and one-half hours at 200°C, followed by a slow anneal to room temperature, respectively. After these thermal treatments, the former sample yielded a spectrum of Lorentzian shape, with $\Delta H = 27$ gauss, while the spectrum of the latter had neither a Gaussian nor a Lorentzian shape. The anisotropy of the resolved hyperfine structure of these spectra remained unchanged.

The experimental results presented here suggest the following possible mechanisms: the resolved hyperfine spectrum of Gaussian shape is caused by two distinct types of paramagnetic centers. Centers of Type I are not affected by thermal treatment, and are responsible for the anisotropic hyperfine structure, which remains unchanged after heating. Centers of Type II are more easily affected by thermal treatments, and are responsible for that part of the resonance that changes in shape from Gaussian to Lorentzian (or from Gaussian to other forms) upon heating. The data suggest that the major part of the Gaussian resonance is caused by centers of Type II.

Table I. Angular dependence of resolved hyperfine structure appearing with ESPR spectra of both Gaussian and Lorentzian shapes which are obtained from irradiated single crystals of LiF.

α	Spacing	Minimum number of resolved lines
0°	14 gauss	19
25°	. . .	No resolved lines
55°	14 gauss	37
72°	7 gauss	45
80°	. . .	No resolved lines
90°	12.5 gauss	17

Since the spin concentrations responsible for the Gaussian resonances of irradiated samples agreed, in order of magnitude, with the *F*-center concentrations in these samples, the Type II center is probably an *F* center. The Type I center may consist of some impurity paramagnetic ion occupying possibly the F^- ion vacancy or perhaps the Li^+ ion vacancy.

Agreement between our resolved hyperfine spectra of Gaussian shape and the spectra of Holton et al. is seen in the 14-gauss spacing of hyperfine lines at $\alpha = 0°$ ($H \parallel [001]$ axis) and at $\alpha = 55°$ ($H \parallel [111]$ axis).

Further investigations appear to be necessary to make all the results compatible.

---

†This research was sponsored by the U. S. Atomic Energy Commission.

*Present address: Department of Physics, Wayne State University, Detroit, Michigan.

[1]W. C. Holton, H. Blum, and C. P. Slichter, Phys. Rev. Letters 5, 197 (1960).

[2]B. S. Gourary and F. J. Adrian, Solid-State Physics, edited by F. Seitz and D. Turnbull (Academic Press, New York, 1960), Vol. 10, p. 128.

[3]Y. W. Kim, R. Kaplan, and P. J. Bray, Bull. Am. Phys. Soc. 3, 178 (1958); 4, 261 (1959); and 5, 252 (1960).

[4]Y. W. Kim, R. Kaplan, and P. J. Bray, Phys. Rev. 117, 740 (1960).

ANOMALOUS NEUTRON DIFFRACTION IN α CADMIUM SULFIDE

S. W. Peterson and H. G. Smith
Chemistry Division, Oak Ridge National Laboratory,* Oak Ridge, Tennessee
(Received December 13, 1960)

The interaction of neutrons with isolated nuclei may be formulated[1] in a general way to include absorption as well as scattering by expressing the scattering length in complex form. The imaginary component of the complex length or amplitude is directly related to the total cross section and is expected to be small except at neutron energies in the neighborhood of a resonance. The energy dependence of the neutron cross section in the resonance region has been given explicitly in the Breit-Wigner dispersion relations. Although the above formulation of neutron scattering is well accepted, a direct experimental demonstration of the imaginary or 90° out of phase scattering component has not previously been given.

Since the phase of scattered radiation is not directly observable, the effect of the imaginary component can be made apparent only through intensity differences caused by interference. Thus, in the Bragg scattering of neutrons from a noncentrosymmetric crystal, the imaginary component from a resonant nucleus can be detected through interference with a real component which is in phase because it originated from nuclei at appropriately displaced sites. A striking result of such interference is a nonequivalence of diffracted intensity from the opposite sides of a diffracting plane; thus $I_{hkl} \neq I_{\bar{h}\bar{k}\bar{l}}$. This result, which is known as a failure or breakdown of Friedel's law,[2] has been frequently observed in the x-ray case and is directly connected with the anomalous scattering which occurs near an absorption edge. The present investigation clearly establishes the corresponding effect for the neutron scattering case and demonstrates a strong energy dependence of the neutron scattering amplitude.

The first evidence for the anomalous scattering effect with neutrons was obtained with cadmium sulfide, chosen because it contains a strong neutron absorber, the Cd^{113} isotope, and crystallizes with a noncentrosymmetric structure. Thin plates of α-CdS, space group $P6mc$, grown from the vapor phase,[3] were used in the majority of the experiments. The experiments consisted of measurement of integrated intensities of (hkl) and $(\bar{h}\bar{k}\bar{l})$ mates of a series of reflections at several wavelengths. The crystallographic phase relations are such that the (004) and (008) pairs should give equal intensities while the (002), (006), and (00, 10) pairs should give unequal intensities for the case where the cadmium scattering amplitude is complex. Figure 1 gives convincing evidence of Friedel's law failure for the latter group of reflections, strongly implying a complex scattering amplitude and hence anomalous scattering.

Figure 2 gives the ratio of $I_{002}/I_{00\bar{2}}$ plotted against wavelength and illustrates the strong

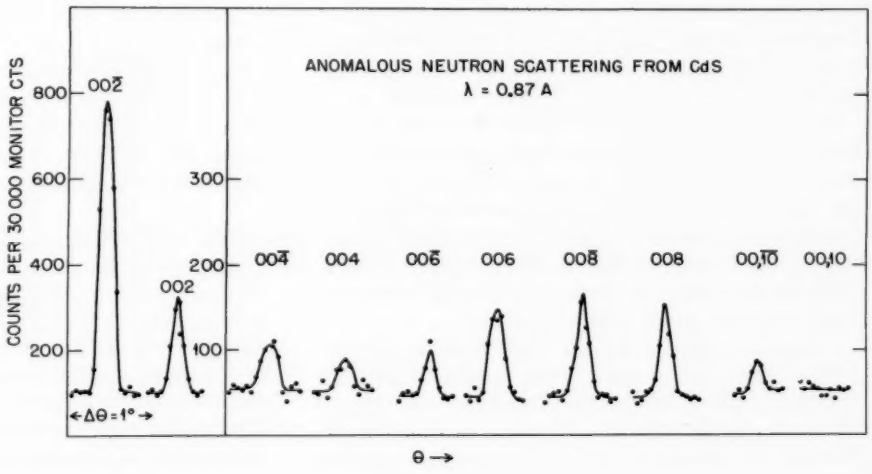

FIG. 1. Neutron diffraction intensities from a single crystal of CdS at $\lambda = 0.87$ A, illustrating nonobservance of Friedel's law in the cadmium resonance region.

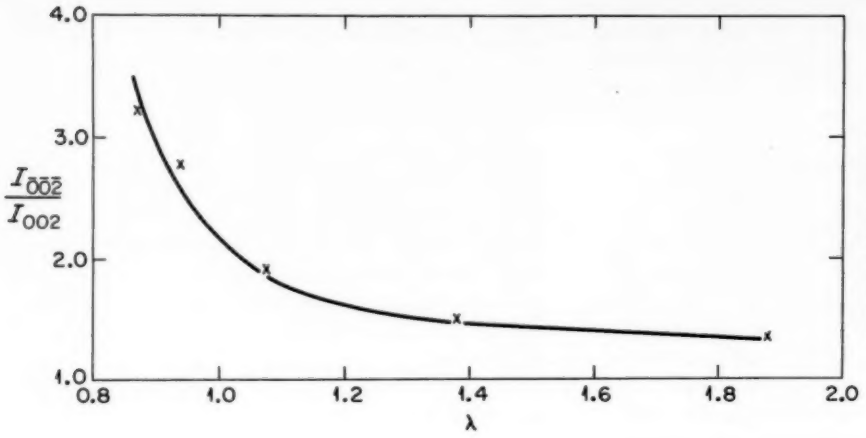

FIG. 2. The wavelength dependence of the intensity ratio $(00\bar{2})/(002)$ of CdS in the cadmium resonance region. The smooth curve is based on the Breit-Wigner formulation. The experimental points are averages of several measurements.

energy dependence of the ratio due to the variation of the complex amplitude of Cd with wavelength. The smooth curve is based on the Breit-Wigner formulation. The coherent scattering amplitude, f, can be expressed in terms of the Breit-Wigner single level parameters in the following way:

$$f = f_0 + \Delta f' + i\Delta f'',$$

where f_0, the nonresonant scattering amplitude, is given approximately by the nuclear radius; the real resonant increment, $\Delta f'$, and the imaginary or 90° phase shifted resonant increment, $\Delta f''$, are

$$\Delta f' = \tfrac{1}{2}\frac{gw\lambda\!\!\!^{-}_0\Gamma_n(E-E_0)}{(E-E_0)^2+\frac{1}{4}\Gamma^2}, \quad \Delta f'' = -\tfrac{1}{4}\frac{gw\lambda\!\!\!^{-}_0\Gamma_n\Gamma}{(E-E_0)^2+\frac{1}{4}\Gamma^2}.$$

Here g is the spin weighting factor, w the isotopic abundance factor, $\lambda\!\!\!^{-}_0$ the wavelength at resonance divided by 2π, Γ_n the neutron width at resonance, Γ the total width, E the energy of measurement, and E_0 the resonance energy.

Table I compares experimental values of $\Delta f'$ and $\Delta f''$ with the calculated ones. The resonance parameters Γ, Γ_n, E_0, and g were taken from the cross-section measurements of Brockhouse.[4] It should be noted that the abundance of Cd^{113} in normal Cd is only 12.3%, which correspondingly reduces the magnitude of the resonance terms in the scattering amplitude.

In order to establish the direction of the phase shift, comparisons were made of the intensity inequalities with both x rays and neutrons for the same crystal of CdS. The result, that the direction of the phase shift is the same for x rays and neutrons (indicated in the diagram below), is in agreement with expectation.

Table I. Cadmium scattering amplitudes in units of 10^{-12} cm.

λ in A	$\Delta f''$ Calc	$\Delta f''$ Obs	$\Delta f'$ Calc	$f_0+\Delta f'$ Calc	$f_0+\Delta f'$ Obs[a]
0.87	0.230	0.21	-0.280	0.34	~0.35
0.94	0.178	0.16	-0.265	0.36	~0.35
1.075	0.125	0.12	-0.238	0.38	~0.40
1.38	0.085	0.08	-0.206	0.41	~0.40
1.88	0.067	0.06	-0.184	0.44	~0.40

[a]A value of $f'(\mathrm{Cd}) = 0.38$ at $\lambda = 1.13$ has been determined previously from powder data of CdO by B. N. Brockhouse and A. T. Stewart according to a private communication.

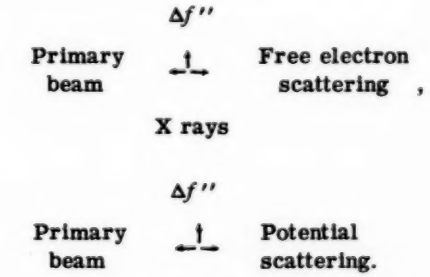

Anomalous x-ray scattering has had important applications in crystallographic work to the determination of absolute configuration[5] and to the direct solution of noncentrosymmetric crystal structures.[6,7] Similar applications of anomalous

neutron scattering are clearly indicated. The potentially useful anomalous scatterers include Li^6, B^{10}, Cd, and a number of examples in the rare earth and actinide series. Experiments are under way to investigate Li^6 and B^{10} as well as several others.

---

*Operated for the U. S. Atomic Energy Commission by Union Carbide Corporation.

[1]See for example O. R. Frisch, Progress in Nuclear Physics (Academic Press, Inc., New York, 1950), Vol. 1, Chap. 8.

[2]R. W. James, The Optical Principles of the Diffraction of X Rays (G. Bell and Sons Ltd., London, 1954), Chap. II, p. 33.

[3]The authors are indebted to D. R. Boyd and Y. T. Sihvonen of the General Motors Research Laboratories for the CdS platelets.

[4]B. N. Brockhouse, Can. J. Phys. 31, 432 (1953).

[5]A. F. Peerdeman, A. J. van Bommel, and J. M. Bijvoet, Proc. Roy. Soc. (Amsterdam) 1354, 16 (1951).

[6]J. M. Bijvoet, Nature 173, 888 (1954).

[7]S. W. Peterson, Nature 176, 395 (1955).

THEORY OF THE PULSATION OF FLUORESCENT LIGHT FROM RUBY

R. W. Hellwarth
Hughes Research Laboratories, Malibu, California
(Received November 17, 1960; revised manuscript received December 8, 1960)

It has been observed[1,2] that when one pumps a ruby crystal placed between two parallel reflecting end plates with intense light in order to create an excess of population in the fluorescent R level(s), there is a threshold of pumping power above which (a) the light from the R line is emitted in pulses accompanied by (b) a sudden spatial and spectral narrowing. This pulsed character of the output is not accounted for by the theory of Schawlow and Townes[3] for a gas Fabry-Perot type maser. We propose here a different approach to this induced fluorescence which predicts that as long as the pump power is above a certain threshold, part of the fluorescent power will occur in recurrent bursts or pulses. From the theory we derive quantitative estimates of the pulse repetition rate, the fraction of power in the pulses, and the nature of the output between pulses, all in terms of the pump power and the ordinary properties of the crystal and end plates. The equations connecting the spectral and spatial narrowing with the time-varying behavior will be developed.

We consider two infinite parallel plates of power reflection coefficient R and a distance d apart. The space between is filled with a ruby crystal. The crystal will be assumed just inhomogeneous enough and the end plates rough enough so that after many internal reflections photons will not interfere in any regular manner; therefore, we may use a straight photon model of the light. Diffraction effects will be assessed in a later article. We shall employ an optically thin crystal which can be pumped uniformly and in which the fluorescent photon density does not vary appreciably across the crystal, i.e., $1-R \ll 1$. To describe the radiation then, we may use the density of photons $u(\nu,\theta)$ traveling in the crystal at a frequency ν from the line-center frequency (measured in units of the half-width at half power) and at an angle θ to the norm. (All photon and population numbers will be measured per unit area of end plate.) We shall assume that we are dealing with a single component of the fluorescent R lines with an approximately $\cos^2\theta$ radiation pattern around a crystal axis that is normal to the end plates. (In an actual apparatus the crystal alignment need not be perfect if the crystal sides are smooth and parallel enough to form a light-pipe between the end plates.) The gain (negative absorption) coefficient $\alpha(\nu,\theta)$ associated with the R line will be assumed to result from a homogeneously broadened line and therefore may be written $[(1+\nu^2)N]^{-1}(n_2-n_1)A\cos^2\theta$ where the peak absorption coefficient A for ruby is commonly of the order 0.4 cm^{-1} at room temperature and 10 cm^{-1} at liquid-nitrogen temperature. We shall measure the level populations and the difference $n=n_2-n_1$ in units of the difference n_0 required for the maser material gain at $\nu,\theta=0$ to just balance the end-plate losses. $n_0=N(1-R)/Ad$. N is the total number of ions (per unit area) which when measured in units of n_0 will be called M. We shall also measure, for convenience, the

photon density $u(\nu, \theta)$ in units of n_0. We may write the time derivative of the photon density as

$$\dot{u}(\nu, \theta) = -u(\nu, \theta)/T(\nu, \theta) + p_i + p_S + D + F, \quad (1)$$

where $T(\nu, \theta)$ is the characteristic decay time of radiation without maser ions present. We shall assume for brevity that T is independent of ν, θ. The nature of the results does not depend much on the behavior of the relaxation times T, especially at wide angles. Then, the value of T to use is evidently $d[c(1-R)]^{-1}$, where c is the velocity of light in the crystal. The induced emission rate p_i will equal $nu(\nu, \theta)\cos^2\theta[(1+\nu^2)T]^{-1}$ with our definitions, and the spontaneous emission rate p_S will be $3n_2 a(\cos^2\theta)[4\pi^2(1+\nu^2)]^{-1}$, where a is the total spontaneous emission probability per second for the R level. The terms D and F represent diffusion of photons from one angle to another and from one frequency to another as a result of crystal and end-plate imperfections, inhomogeneous broadening, and "spin-spin" interactions, etc. It has been estimated that these effects are not large enough to alter the character of the results and a discussion of them will be deferred. The time derivative of the population difference is given by

$$\tfrac{1}{2}\dot{n} = P_p - P_S - \int_{-\infty}^{\infty} d\nu \int_0^{\pi} d\theta \, \sin\theta \, p_i(\theta, \nu). \quad (2)$$

The crystal absorbs P_p pump photons per second (per unit area per n_0) and spontaneously emits P_S maser photons per second. The net contribution to the derivative of n from these terms is $\frac{1}{2}(w-a)M - \frac{1}{2}(w+a)n$, where w is the pump transition probability per second. The last term of (2) is the integrated induced transition rate. When $n<1$, the natural exponential decay time for the photon density is of the order T, which is roughly a million times shorter than any of the time constants for the decay of the populations which are of order $(wM)^{-1}$. Therefore, for $n<1$, the photon density follows very accurately and quickly any change in n, and we may use the adiabatic solution of (1) for the radiation (which reduces to the quiescent solution when n is constant):

$$\frac{u(\nu, \theta, t)}{T} \approx \frac{3(M+n)a\cos^2\theta}{8\pi^2[1+\nu^2 - n(t)\cos^2\theta]}, \quad (n<1). \quad (3)$$

If we integrate Eq. (3) over solid angle and frequency, we obtain the total output flux of photons $P_0[n(t)]$:

$$P_0[n(t)] = \tfrac{3}{4}a(M+n)[\sin^{-1}n^{1/2} - (n-n^2)^{1/2}]n^{-3/2}. \quad (4)$$

The differential equation for n in the region where the radiation can react so quickly is

$$\tfrac{1}{2}\dot{n} = P_p(n) - P_0(n), \quad (5)$$

and n changes so as to approach a value such that $P_p = P_0$. However, if in (4) we let n approach 1, P_0 approaches the value $\frac{3}{4}\pi a(M+1)$, and since clearly no quiescent solution exists for $n>1$, we have an upper limit on the output photon flux P_0 in the quiescent state. Since the output photon flux must equal the input flux from the pump (on the average), we know the pump rate w at which $n=1$, which we call the threshold pump rate w_0. For the simplifications we have made, $w_0 = 3\pi a/4$; for more accurate assumptions it is less. For $w>w_0$ we have to solve the infinite set of coupled equations (1) for $u(\nu, \theta, t)$ (one equation for each value of θ) together with Eq. (2) for the populations. Since this set is nonlinear we must proceed by approximation, the easiest method of which is to break time into intervals in which different terms may be taken as dominating, and then to connect the solutions in each interval as follows.

If the pump power is turned on suddenly so that $w>w_0$, then the population increases according to (6) until $n=1$. For a short time thereafter, of the order of $(T/wM')^{1/2}$, n continues increasing beyond unity at about the same rate as at $n=1$ to a value of the order $(wM'T)^{1/2}$ above unity. $M' \equiv M(1-w_0/w)$. At this point the positive exponential blowup of radiation quickly takes over. This wipes out the excess of n above unity by induced emission, creating momentarily $\sim\frac{1}{2}(wM'T)^{1/2}$ photons. The photon density decays in roughly Gaussian fashion, with the total decay rate being impeded by the production of more stimulated photons, and this drives n to a value $\epsilon \sim (wM'T_0)^{1/4}$ below 1 in a time $\sim T(wM'T)^{-1/4}$. By this time the photon density has locked P_0 to the value given by (4); n recommences its relatively slow recovery toward 1, and the whole process repeats cyclically. We may integrate (4) to find the recovery time between pulses, i.e., the time for n to grow from $1-\epsilon$ to 1. For any realizable pump probability w, we see that $\epsilon \ll 1$ and we may use this approximation to simplify the inte-

gration and obtain for the recovery time T_γ, ($W \equiv w/w_0$)

$$T_\gamma \approx \frac{\pi}{w_0 M(1+\sqrt{2})}\left[\epsilon^{1/2} - \frac{(W-1)\pi}{(1+\sqrt{2})2}\ln\left(1+\frac{2(1+\sqrt{2})}{\pi(W-1)}\epsilon^{1/2}\right)\right]. \quad (6)$$

A plot of $T_\gamma w_0 M$ versus W is shown in Fig. 1 with the spontaneous lifetime $a = 3\times10^{-3}$ sec, $R = 0.95$, $d = 1$ cm, and for the values $A = 0.4$ and 10 cm^{-1}. Despite the great simplifications, the results of (6) are in good agreement with the rough preliminary experimental results (giving for example $T_\gamma \approx 8$ μsec for $W = 2$ and $A = 0.4$ cm^{-1}). Fortunately the errors made in estimating ϵ fall under the fourth or eighth root and contribute correspondingly little to the error of (6).

Among the implications of the foregoing estimates of the behavior of populations and the output power for noninterfering fluorescence with negligible photon diffusion are the following: (a) If $T(\nu,\theta)\alpha(\nu,\theta)$ has a maximum in direction (and frequency) so that the total integrated output, computed from (1) with $\dot{u} = 0$ and infinite gain in the optimum direction, is finite, then there is a threshold at this output power above which pulses may be expected to appear continuously. (b) The fraction of the total output light that is emitted during the pulses is significant and is approximately $(wM'T)^{1/4}(wMT_\gamma)^{-1}$. This is of the order $\frac{1}{4}$ at $W \sim 1.1$ and approaches $(W-1)/W$ at high W. (c) Our estimate of $n(t)$ may be inserted into Eq. (1) to solve for the detailed behavior of the radiation as a function of time, frequency, and angle. The entire calculation seems too difficult without machine computation. However, the average narrowing factor during the interval between pulses has been estimated to be of the order $[Mw_0T(W-1)]^{1/8}$ both for spatial narrowing over the $\cos^2\theta$ behavior and for frequency narrowing over the natural linewidth. During the pulse the spatial narrowing is evidently great enough that interference and diffusion effects might alter the prediction of (1) for the spatial distribution significantly.

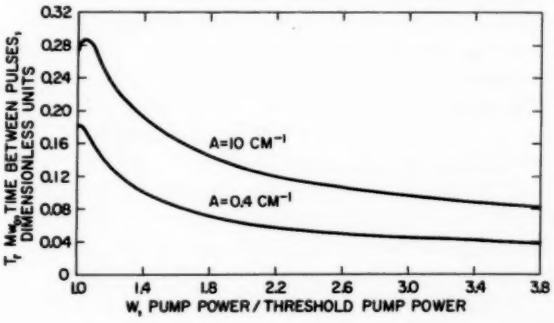

FIG. 1. Two plots of Eq. (6) for the time elapsed between pulses T_γ as a function of pump power each with $d = 1$ cm, $R = 0.95$, and $a = 3\times10^{-3}$ sec, but with different room temperature absorption coefficient A. The dimensionless units chosen make the function insensitive to changes in the above parameters.

Statz and deMars[4] have explained the possibility of a pulsed output in the simpler case of a single-mode microwave ruby maser. However, that the results of this paper differ quantitatively from those that would be obtained using the equations of Statz and deMars with new parameters appropriate to the optical case rests essentially on two things: (a) We have assumed that photons may propagate in any of a continuum of directions, which requires the "continuum" of equations of (1) and (2) rather than the two coupled equations of reference 4. Also, Eqs. (1) and (2) cannot be reduced to the form of two coupled equations in two variables. (b) Our threshold for pulsations depends on the anisotropy of the propagation constant α for ruby, or more precisely on the curvature at maximum of $\alpha(\nu,\theta)T(\nu,\theta)$. This threshold increases as the anisotropy is diminished to where, for the isotropic gas maser described by Townes and Schawlow, it might well be too high to be significant experimentally. Also for a gas maser, the medium is so much more optically homogeneous that interference phenomena would play a dominant role and the approach of Townes and Schawlow would be more direct than a modification of the approach presented here.

I would like to thank T. H. Maiman for valuable discussions of experimental results and G. Birnbaum for his interest and encouragement.

---

[1]R. J. Collins, D. F. Nelson, A. L. Schawlow, W. Bond, C. G. B. Garrett, and W. Kaiser, Phys.

Rev. Letters 5, 303 (1960).
[2]T. H. Maiman, report at the 1960 Annual Meeting of the Optical Society of America, Boston, Massachusetts, 1960, ATCl.
[3]A. L. Schawlow and C. H. Townes, Phys. Rev. 112, 1940 (1958).
[4]H. Statz and G. deMars, Quantum Electronics (Columbia University Press, New York, 1960).

ANGULAR DISTRIBUTION OF LYMAN-α RADIATION EMITTED BY H (2S) ATOMS IN WEAK ELECTRIC FIELDS

William Lichten
Department of Physics, Ryerson Laboratory, University of Chicago, Chicago, Illinois
(Received November 22, 1960)

H atoms in the 2S state are known to be metastable in a field-free region.[1] Application of an electric field perturbs the atoms, causing them to emit Lyman-α radiation and to decay to the 1S ground state. It is the purpose of this Letter to point out that the angular distribution of the radiation is isotropic and to examine the consequences of this conclusion for interpretation of certain electron-scattering experiments.

The electric-field-induced emission process can be considered as arising from a perturbation of the $2\,^2S_{1/2}$ state by the nearby $2\,^2P_{1/2}$ levels only. Since the $2\,^2P_{3/2}$ levels are energetically much farther away from 2S, their effect can be neglected. The effect of the perturbation of each $P_{1/2}$ level can be considered separately unless the coupling by the electric field is too strong, or unless there is accidental level crossing.[2] If one assumes that the latter condition is not present, the former can occur only if the perturbing matrix element V is comparable to the energy separation $h\nu$ between the $S_{1/2}$ and $P_{1/2}$ levels. Here $\nu = [E(S_{1/2}) - E(P_{1/2})]/h \sim 10^9$ cps; $V/h \sim ea_0E/h \sim 10^8$ cps for a typical laboratory quenching field of 50 v/cm, and the condition of weak coupling is well fulfilled.

Thus, it is only necessary to consider separately the angular distribution of the radiation emitted by an H atom in either of the two $P_{1/2}$ states. The well-known formulas[3] for the relative strengths of the π and σ lines give

$$I(\pi)/I(\sigma) = 4m^2/(J \pm m)(J \mp m + 1).$$

In the present case $J = \frac{1}{2}$, $m = +\frac{1}{2}$, and $I(\pi)/I(\sigma) = 1$. Thus the radiation is completely unpolarized and the angular distribution is isotropic.

Recently a controversy has arisen over the absolute magnitude of the cross section $\sigma(2S)$ for excitation of the 2S state of H by electron impact. Schultz and the writer[4] measured $\sigma(2S)$ from threshold (10.2 ev) to about 45 ev. The maximum value for $\sigma(2S)$ was $(0.35 + 0.05)\pi a_0^2$. Since the results depended primarily on normalization of the data to the Born approximation, the conclusions are unaffected by the present paper. A considerably less precise confirmatory absolute determination measured the number of photons emitted by electrostatic quenching. Since, in the latter experiment, the data were treated by assuming isotropic angular distribution of the photons, the conclusions of Schultz and the author rest unchanged.

Subsequently, Fite and co-workers[5] have measured $\sigma(2S)$ by comparing the intensity of photons emitted from quenched H (2S) atoms with the intensity arising from excited 2P atoms. [$\sigma(2P)$ had been measured previously by normalization to the Born approximation.] The measured $\sigma(2S)$ was consistently about one third of the results of Schultz and the writer over the common energy range. Fite et al. extended the observations to energies as high as 700 ev. Above 300 ev, the results agreed with the Born approximation. Fite et al. stated that this agreement was "thought to be undeniable evidence" for the correctness of the lower value for $\sigma(2S)$.

However, Fite et al. assumed 100% polarization of the radiation parallel to the electric field and perpendicular to the direction of observation. They multiplied their results by a factor of 2/3 to correct for anisotropy. According to the result of the present paper, this correction should not be made, since the radiation is isotropic. Thus the results of Fite et al. should be raised by 50%. This would bring their maximum cross section to $0.16\pi a_0^2$, in better agreement with the higher value of Schultz and the writer. Nevertheless, the disagreement is still substantial and exceeds the combined errors.

The most probable values of Fite et al. now

exceed the Born approximation by 50% above 300 ev. Their results agree fairly well with a calculation by Marriott.[6] However, very recently Smith[7] has pointed out that the partial wave analysis of Marriott omitted important p- and d-wave contributions. When these and other terms are included, the calculations of Smith[7] are in disagreement with the results of Fite et al. The new theoretical results agree with the measurements of Schultz and the writer within the quoted experimental error.

[1]The properties of the $n=2$ level of H are discussed in the well-known work of Lamb and co-workers. For a summary and bibliographic references, see N. F. Ramsey, Molecular Beams (Oxford University Press, New York, 1956), Chap. 12.

[2]F. D. Colegrove, P. A. Franken, R. R. Lewis, and R. H. Sands, Phys. Rev. Letters 3, 420 (1959).

[3]E. U. Condon and G. H. Shortley, The Theory of Atomic Spectra (Cambridge University Press, London, 1953), p. 387. Strictly speaking, the effect of the hyperfine interaction should be taken into account. However, magnetic interactions of this type always have a depolarizing effect, so the result will be unchanged.

[4]W. Lichten and S. Schultz, Phys. Rev. 116, 1132 (1959).

[5]R. F. Stebbings, W. L. Fite, D. G. Hummer, and R. T. Brackmann, Phys. Rev. 119, 1939 (1960).

[6]R. Marriott, Proc. Phys. Soc. (London) 72, 121 (1958).

[7]K. Smith, Phys. Rev. 120, 845 (1960).

10-Mev PROTON REACTION CROSS SECTIONS FOR Cu^{63} AND Cu^{65}†

Richard D. Albert and Luisa F. Hansen
Lawrence Radiation Laboratory, University of California, Livermore, California
(Received November 18, 1960)

Recently, Meyer and Hintz[1] have reported results obtained on the reaction cross sections, σ_R, for several nuclei (including Cu^{63} and Cu^{65}) with incident protons of 9.85 Mev. The results were obtained using the following relation for σ_R:

$$\sigma_R = \sigma(p,q) + \sigma(p,n), \qquad (1)$$

where $\sigma(p,q)$ is the sum of the (p,p') and (p,α) cross sections which they have measured, and $\sigma(p,n)$ is a weighted sum of (p,n) cross sections which others have measured.[2-5] The expression (1) for σ_R neglects contributions from proton capture and compound elastic scattering which are believed to be small at this energy. Other reactions including multiple particle emission are either energetically forbidden or greatly reduced by the Coulomb barrier.

These authors[1] find that the proton reaction cross sections they obtain using expression (1) are significantly larger than the optical model calculations obtained using parameters that fit proton elastic scattering and polarization measurements. This is a strong statement since, as they point out, the reaction cross sections obtained with (1) are always lower limits. They also find that the two copper isotopes Cu^{63} and Cu^{65} have considerably different reaction cross sections (845^{+92}_{-67} and 974 ± 76 millibarns, respectively). This is difficult to justify using optical model theory which predicts them to be nearly the same. They feel that this difference may not be real but rather due to large errors in the (p,n) measurements.

We have recently measured (p,n) cross sections for Cu^{63} and Cu^{65} using variable energy protons from the Livermore 90-in. cyclotron and detecting neutrons by a "long counter" technique previously described.[6] Targets were in the form of metallic foils approximately 1.5 mg/cm² thick.

We obtain (p,n) cross sections for Cu^{63} and Cu^{65} at 9.85 Mev (510 and 700 millibarns, respectively) which differ appreciably from the weighted sums (480^{+90}_{-65} and 819 ± 75 millibarns, respectively) used by Meyer and Hintz.[1] The estimated absolute error in these (p,n) cross sections is 7%. When these (p,n) cross sections are combined with the (p,q) cross sections of Meyer and Hintz[1] [measurements by Benveniste, Booth, and Mitchell[7] of this laboratory agree within the errors quoted with these (p,q) cross sections], we obtain for the reaction cross sections, σ_R, of Cu^{63} and Cu^{65}, 875 and 855 millibarns, respectively. These agree within a few percent as predicted by the optical model.

Our results were compared with a surface-absorption optical-model calculation of Bjorklund

and Fernbach[8] which used parameters obtained by fitting proton elastic scattering and polarization data. These parameters are: radius constant, $r_0 = 1.25$ fermis; real potential, $V = 51$ Mev; imaginary potential, $W = 11$ Mev; and diffuseness parameter, $a = 0.65$ fermis. The spin-orbit potential used was 20 times the Thomas term. This yielded a reaction cross section, $\sigma_R = 805$ millibarns.[9] Considering the experimental errors, we feel that the experimental results we obtain for these nuclei do agree with surface-absorption optical-model calculations.

Reaction cross sections of a number of other nuclei are being determined by this method. Preliminary results for 10-Mev protons are in reasonable agreement with surface-absorption optical-model calculations, using parameters that fit polarization and elastic scattering, over a wide region of the periodic table.

†Work was performed under the auspices of the U. S. Atomic Energy Commission.

[1]V. Meyer and N. M. Hintz, Phys. Rev. Letters 5, 207 (1960).
[2]S. N. Ghoshal, Phys. Rev. 80, 939 (1950).
[3]J. P. Blaser, F. Boehm, P. Marmier, and D. C. Peaslee, Helv. Phys. Acta 24, 441, 465 (1951).
[4]H. A. Howe, Phys. Rev. 109, 2083 (1958).
[5]H. G. Blosser and T. H. Handley, Phys. Rev. 100, 1340 (1955).
[6]Richard D. Albert, Phys. Rev. 115, 925 (1959).
[7]J. Benveniste, R. Booth, and A. Mitchell (private communication).
[8]F. Bjorklund and S. Fernbach, Phys. Rev. 109, 1295 (1958).
[9]F. Bjorklund (private communication).

DECOUPLING OF A TIME-DEPENDENT PERTURBATION CAUSED BY AFTEREFFECTS OF HOLE FORMATION

B. -G. Pettersson, T. R. Gerholm, J. Thun, and K. Siegbahn
Institute of Physics, University of Uppsala, Uppsala, Sweden
(Received November 7, 1960)

It has been suggested[1] that the aftereffects caused by the formation of a hole in one of the electron shells by electron capture or internal conversion might give rise to a time-dependent magnetic coupling between the electron shell and the nucleus. Such a coupling, if it exists, should affect the angular correlation between successive nuclear radiations, resulting in a more or less complete wipeout of the angular correlation pattern. Experimental studies of this effect have led to confusing results. Some experimenters[2] claim to have found evidence for the aftereffects of hole formation. Even a completely isotropic correlation has been reported.[3] Others,[4-6] however, have been led to the conclusion that there is no observable attenuation caused by the aftereffects.

The main reason for this disagreement is probably due to the interference between the eventual hole effect and the simultaneously present quadrupole interaction. The latter also gives an attenuation due to the coupling between the nuclear quadrupole moment, eQ, and the crystalline electric field gradients $\partial E/\partial z$. It is possible, however, to separate the two effects by means of delayed angular correlation experiments. Abragam and Pound[7] have shown that the quadrupole attenuation can be described by means of attenuation factors $G_{2\nu}$. The angular correlation is then given by

$$W(\theta, t) = 1 + G_2(t)A_2P_2(\theta) + G_4(t)A_4P_4(\theta). \qquad (1)$$

For $G_2(t)$ one has for spin 5/2 of the intermediate level

$$G_2(t) = \tfrac{1}{5}\,(1 + \tfrac{13}{7}\cos\omega_0 t + \tfrac{10}{7}\cos 2\omega_0 t + \tfrac{5}{7}\cos 3\omega_0 t),$$

where ω_0 is the ground precession frequency and t is the time delay. In the case of delayed angular correlations the actually observed $\overline{G}_2(t)$ becomes a weighted mean of $G_2(t)$ for the time range in question determined by the resolving time of the coincidence circuit. $\overline{G}_2(t)$ can be evaluated by integrating over (1). The delayed angular correlations can then be used to determine the strength of the quadrupole interaction. An additional attenuation, which cannot be accounted for by the quadrupole interaction mechanism is then, presumably, due to the aftereffects.

For our experiment we have chosen the 165-kev conversion electron 134-kev gamma cascade in Hg^{197m}. The intermediate level has a mean life of 9×10^{-9} sec,[8] which allows for delayed angular correlations and still is sufficiently short to permit a reasonable competition between the quad-

rupole and magnetic couplings.

In an extensive series of measurements[9] we have studied this correlation for varying source conditions. Sources were produced by bombarding gold with 18-Mev protons and the Hg^{197m} activity was vacuum-evaporated onto the backing material which was cooled with liquid air. Thus it was possible to vary the source environment by choosing different backing materials. Four metallic environment backings of Ag, Au, Al, and Ga were used. Four different insulators were used, namely: rubber hydrochloride, Mylar, Mg oxide, and Al oxide. In Fig. 1 are given the calculated quadrupole attenuation factors $\overline{G}_2(t)$ for the three different delay positions used. The attenuations observed are in complete agreement with the theory for all metallic sources. For insulating source environment, however, we were forced to assume an additional attenuation mechanism. The ratio of the A_2 coefficients measured in the fast, normal, and delayed positions are compatible with a pure quadrupole interaction mechanism. However, the absolute values show an additional attenuation of a fast "on-off" character present immediately after the K conversion. Thus we may write $\overline{G}_2(\text{fast}) = \overline{G}_2(\text{hole}) \times \overline{G}_2(Q, \text{fast})$. As shown in the insert of Fig. 1, we can use the ratio of $\overline{G}_2(\text{normal})/\overline{G}_2(\text{delayed})$ to predict $\overline{G}_2(Q, \text{fast})$ which is then to be compared with the experimentally measured $\overline{G}_2(\text{fast})$. In this way $\overline{G}_2(\text{hole})$ is determined. The four different insulating source environments, mentioned above, all gave the same results, namely, $\overline{G}_2(\text{hole}) = 0.70$.

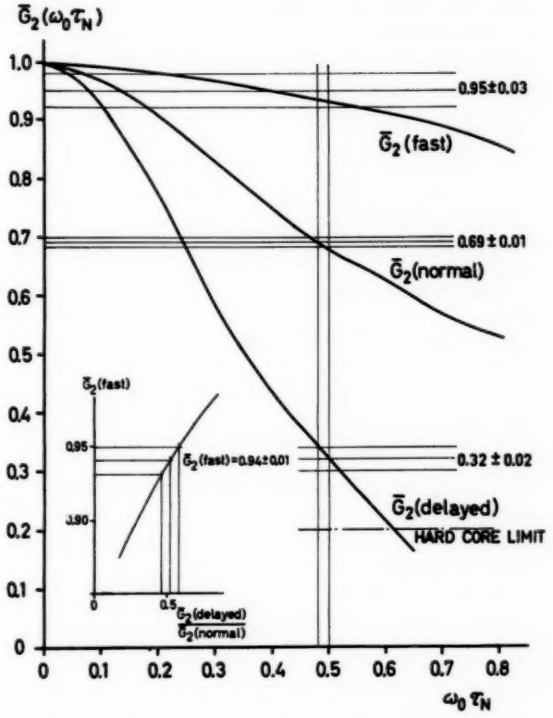

FIG. 1. $\overline{G}_2(\omega_0\tau_N)$ as a function of the strength of the quadrupole coupling, $\omega_0\tau_N$, for the three different delay positions used. The experimental results given in the figure correspond to correlations measured with an Au backing. Insert: Results for a rubber hydrochloride backing; $\overline{G}_2(\text{delayed})/\overline{G}_2(\text{normal})$ corresponds to a theoretical $\overline{G}_2(\text{fast}) = 0.94 \pm 0.01$ to be compared with the experimentally obtained value 0.66 ± 0.04, thus indicating an additional attenuation $G_2(\text{hole}) = 0.70 \pm 0.05$.

These results are consistent with an aftereffect mechanism. For metallic sources the total recovery time is supposed to be very short ($\lesssim 10^{-14}$ sec) because of the availability of conducting electrons to neutralize the ion. For insulators, however, it is conceivable that the atom can remain in a highly ionized state for an appreciable time. The unpaired electron spins in the outermost orbits then give rise to a magnetic coupling which may be quite large. To exclude the possibility that the attenuation observed for insulator source-backings is due to the charging up of the source, we measured the 130 kev - 279 kev electron-gamma correlation in Au^{197} where the mean life of the intermediate level, 2.3×10^{-11} sec, is too short to give any attenuation due to extra nuclear fields. No difference between metallic and insulator backings was observed in this case.

To prove our aftereffects hypothesis for insulator source-backings, we have performed a magnetic decoupling experiment. (See Fig. 2.) The source was exposed to a fairly strong (≈ 3000 gauss) magnetic field parallel to the direction of emission of the conversion electrons. The nuclear spin I and the electron spin J then precess around the field axis. The attenuation is thus removed and the resulting angular correlation should be affected by the quadrupole interaction only. There is a slight complication due to the fact that the correction factor, f, for the finite aperture of the electron channel (a magnetic beta-ray spectrometer) depends on the focussing action of the field produced by the decoupling magnet. The appropriate expressions become, for the 180° position used in our experiment,

$$W_0(\text{metal}) = 1 + f_0\,\overline{G}_2(Q, \text{metal})\,A_2,$$

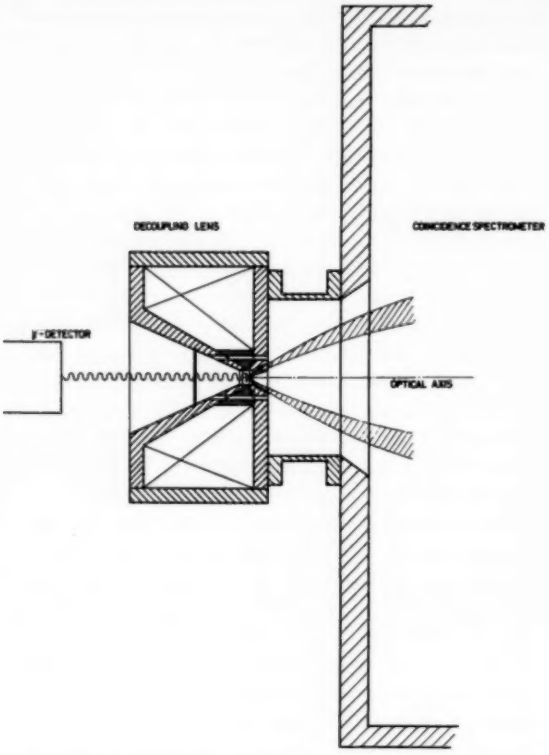

FIG. 2. Magnet used for the decoupling experiment.

$$W_B(\text{metal}) = 1 + f_B \bar{G}_2(Q, \text{metal}) A_2,$$

$$W_0(\text{insul}) = 1 + f_0 \bar{G}_2(\text{hole}) \bar{G}_2(Q, \text{insul}) A_2,$$

$$W_B(\text{insul}) = 1 + f_B \bar{G}_2(Q, \text{insul}) A_2,$$

and

$$A_2(\text{measured}) = f_0 \bar{G}_2(Q) \bar{G}_2(\text{hole}) A_2,$$

determined from an angular correlation measurement on the source used.

The geometrical correction factor f_B was determined for several different metallic sources with different quadrupole interaction couplings. For a given magnetic field, B, the factors f_B thus determined were found to be equal and in agreement with a theoretically calculated value based on the observed increase of the single counting rate in the electron channel. The experiments were performed in the "normal" delay position, where the angular correlation gave $\bar{G}_2(\text{hole}) = 0.70 \pm 0.03$ and $\bar{G}_2(Q) = 0.70 \pm 0.05$. From the coincidence counting rates divided by the electron single counting rates, we obtained from the relations above, for $f_0 = 0.80$ and $A_2 = 0.20$: $\bar{G}_2(\text{hole}) = 0.71 \pm 0.03$ and $\bar{G}_2(Q) = 0.70 \pm 0.05$, in perfect agreement with the angular correlation results. The magnetic decoupling experiment proves the existence of a time-dependent perturbation caused by the aftereffects of hole formation and confirms the conclusions drawn from our delayed coincidence experiments.

[1]H. Frauenfelder, Phys. Rev. 82, 549 (1951).
[2]F. Gimmi, E. Heer, and P. Scherrer, Helv. Phys. Acta 29, 147 (1956).
[3]E. Breitenberger, Proc. Phys. Soc. (London) A69, 566 (1956).
[4]E. S. Snyder and S. Frankel, Phys. Rev. 106, 755 (1957).
[5]N. Goldberg and S. Frankel, Phys. Rev. 100, 1350 (1955).
[6]H. H. Coburn, J. V. Kane, and S. Frankel, Phys. Rev. 105, 1293 (1957).
[7]A. Abragam and R. V. Pound, Phys. Rev. 92, 943 (1953).
[8]T. Suter, P. Reyes-Suter, and T. R. Gerholm, Arkiv Fysik (to be published).
[9]B. -G. Pettersson, J. Thun, and T. R. Gerholm (to be published).

STUDY OF NUCLEAR STRUCTURE FROM COULOMB ENERGY DIFFERENCES OF MIRROR LEVELS*

K. Wildermuth and Y. C. Tang
Florida State University, Tallahassee, Florida
(Received November 9, 1960; revised manuscript received December 9, 1960)

One of the assertions of the cluster model of atomic nuclei is that the cluster structure can change from level to level in the same nucleus.[1,2] Recent analyses on the energy spectra and gamma transition probabilities of light and medium-weight nuclei seem to support this viewpoint.[3] For instance, in the case of He^5, it was found that the ground state has an alpha-neutron configuration, while the $(\frac{3}{2}+)$ excited state is best described by a deuteron cluster and a triton cluster in relative motion.[4] As the charge distribution of a nucleus is directly related to the wave function which describes the state in question, one would expect that the cluster structure will affect the Coulomb energy to a considerable extent. Therefore, by studying the Coulomb energy behavior from the energy spectra in mirror nuclei, one might gain some information about the cluster structures of the levels; this is so, since the influence of the nuclear forces is the same in corresponding mirror levels.

To see this in more detail, we consider as a special example the three lowest energy levels of the mirror pair F^{19} and Ne^{19}.[5] (See Fig. 1.) From detailed studies on the energy spectra, it was concluded[1] that the cluster structure of the $(\frac{1}{2}+)$ and $(\frac{5}{2}+)$ levels of F^{19} (Ne^{19}) is described by an unexcited O^{16} cluster and a triton (He^3) cluster in relative motion of orbital angular momentum $L=0$ and $L=2$. These two levels are, therefore, members of a rotational band,[6] and we expect that the Coulomb energies should be approximately the same in both of these levels. Experimentally, we indeed find that the excitation energies of the $(\frac{5}{2}+)$ levels are nearly the same in both F^{19} and Ne^{19}. For the $(\frac{1}{2}-)$ levels, we have, however, a different situation. These levels are best described[1] by an unexcited N^{15} (O^{15}) cluster and an alpha cluster in relative oscillation of angular momentum $L=0$. To get the configuration of those states from that of the ground states, one moves a proton from the O^{16} core in F^{19} and a neutron from the O^{16} core in Ne^{19}. Together with the outside triton or He^3 cluster, an alpha cluster is then formed. This means that there is a decrease of Coulomb energy for F^{19}, but not for Ne^{19} in first approximation. Therefore, one has to expect that the $(\frac{1}{2}-)$ level in Ne^{19} has a considerably larger excitation energy than the corresponding level in F^{19}. Experimentally, this is indeed the case.

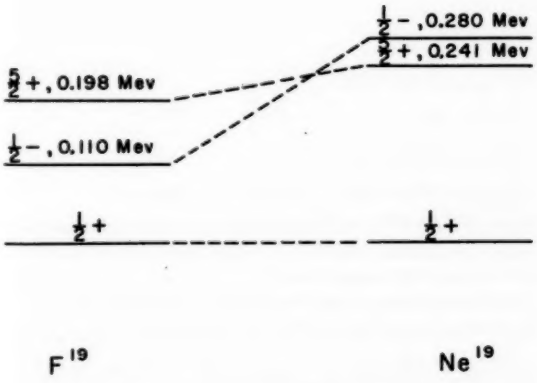

FIG. 1. Energy spectra of F^{19} and Ne^{19}.

For a crude estimate, we write

$$\Delta E \equiv E_{\mathrm{Ne}}^{\mathrm{exc}}(\tfrac{1}{2}-) - E_{\mathrm{F}}^{\mathrm{exc}}(\tfrac{1}{2}-)$$

$$\approx \Delta E(O^{15}-N^{15}) - \Delta E(He^3-H^3) - (9e^2/R_{\mathrm{F}})(1-\tfrac{1}{5}R_{\mathrm{O}}^{\,2}/R_{\mathrm{F}}^{\,2}), \quad (1)$$

where $E_{\mathrm{Ne}}^{\mathrm{exc}}(\frac{1}{2}-)$ and $E_{\mathrm{F}}^{\mathrm{exc}}(\frac{1}{2}-)$ are the excitation energies of the $(\frac{1}{2}-)$ levels in Ne^{19} and F^{19}, respectively. The expressions $\Delta E(O^{15}-N^{15})$ and $\Delta E(He^3-H^3)$ represent the Coulomb energy differences of O^{15} and N^{15}, and of He^3 and H^3. Finally, R_{F} and R_{O} denote the radii of F^{19} and O^{16}, respectively. To obtain the above expression, we have made the crude approximation that the charge distribution in which the above-mentioned proton moves can be represented by the following expression:

$$\rho(r) = \frac{3e}{4\pi}\left(\frac{7}{R_{\mathrm{O}}^{\,3}} + \frac{1}{R_{\mathrm{F}}^{\,3}}\right) \quad \text{for } r \le R_{\mathrm{O}}$$

$$= 3e/4\pi R_{\mathrm{F}}^{\,3} \quad \text{for } R_{\mathrm{O}} \le r \le R_{\mathrm{F}}. \quad (2)$$

Furthermore, we have assumed that the $(\frac{1}{2}-)$

state of F^{19} has the same radius R_F as that of the ground state and that the alpha cluster has a constant probability distribution over the volume $V=(4\pi/3)R_F^3$. Taking the value of R_F as calculated from the Coulomb energy differences of the ground states of Ne^{19} and F^{19} and adopting the experimental values of $\Delta E(O^{15}-N^{15})$, $\Delta E(He^3-H^3)$, R_O,[7] we can then calculate ΔE. This turns out to be 0.21 Mev; experimentally, it is 0.17 Mev.

For all the mirror levels of which one knows their cluster structures, one can calculate in a similar way the above-mentioned excitation energy differences ΔE. In Table I, we list a number of such examples. It is seen that the agreement between the calculated and experimental values is fairly good. In particular, the sign of ΔE is always predicted correctly. For levels which are in the same rotational band with the ground state, the magnitude of ΔE is always smaller than 0.1 Mev. From our arguments presented in the previous paragraphs, this should indeed be expected.

Recent experiments seem to indicate that the excitation energy of the $(\frac{3}{2}+)$ level in Li^5 is 16.64 Mev,[8] instead of 16.81 Mev previously listed.[5] If this is indeed so, then ΔE would be negative in contradiction to our prediction from the assumed cluster structure of this level. As there is at the present moment ample evidence[4,5] favoring a deuteron cluster plus a triton cluster configuration for this state, we expect that this apparent discrepancy comes from the fact that it is rather difficult to determine to a good accuracy the energies of the ground states of He^5 and Li^5 because of the extreme widths of these states.

Finally, we wish to mention that one can also go the other way; that is, from the ΔE value of mirror levels, one can also learn about the cluster structure. For example, let us consider briefly the $(\frac{1}{2}-)$ levels of the mirror pair F^{17} and O^{17} at excitation energies of 3.10 and 3.06 Mev, respectively. If these levels could be described by the excitation of the outside nucleon into a higher shell, then we would have to expect that the $(\frac{1}{2}-)$ level in F^{17} has an appreciably lower excitation energy than the corresponding level in O^{17} (about 0.5 Mev). Experimentally, this is, however, not at all the case. Therefore, one has to assume for the cluster structure of these mirror levels essentially an alpha-particle excitation of the O^{16} cluster core. Although the lowest excitation of this kind in O^{16} needs an energy of 6.06 Mev, one can account for the decrease of the excitation energy in F^{17}

Table I. Excitation energy differences of mirror levels.

Nuclear levels	Excitation energy (Mev)	Cluster structure[a]	Cluster structure of ground state	ΔE_{exp} (Mev)	ΔE_{theor} (Mev)	Remarks
$Li^5(He^5)$, $\frac{3}{2}+$	16.81(16.69)	$He^3(H^3)$-d, $2s$	α-$p(n)$, $1p$	+0.12	+0.12	b
$Be^7(Li^7)$, $\frac{1}{2}-$	0.431(0.478)	$He^3(H^3)$-α, $2p$	$He^3(H^3)$-α, $2p$	-0.05	$\lesssim 0$	c
$Be^7(Li^7)$, $\frac{7}{2}-$	4.54(4.63)	$He^3(H^3)$-α, $1f$	$He^3(H^3)$-α, $2p$	-0.09	-0.06	b, c
$Be^7(Li^7)$, $\frac{5}{2}-$	7.18(7.47)	Li^6g.s.-$p(n)$, $1p$	$He^3(H^3)$-α, $2p$	-0.29	-0.36	
$C^{11}(B^{11})$, $\frac{1}{2}-$	1.99(2.13)	Be^8g.s.-$He^3(H^3)$, $2p$	Be^8g.s.-$He^3(H^3)$, $2p$	-0.14	$\lesssim 0$	
$N^{13}(C^{13})$, $\frac{1}{2}+$	2.37(3.09)	C^{12}g.s.-$p(n)$, $2s$	C^{12}g.s.-$p(n)$, $1p$	-0.72	-0.60	d
$Ne^{19}(F^{19})$, $\frac{1}{2}-$	0.28(0.11)	O^{15}g.s.(N^{15}g.s.)-α, $5s$	O^{16}g.s.-$He^3(H^3)$, $4s$	+0.17	+0.21	
$Ne^{19}(F^{19})$, $\frac{5}{2}+$	0.241(0.197)	O^{16}g.s.-$He^3(H^3)$, $3d$	O^{16}g.s.-$He^3(H^3)$, $4s$	+0.04	≈ 0	c

[a]In this column, we list the internal structures and the modes of relative motion. For instance, the $(\frac{3}{2}+)$ level of He^5 is described by a deuteron cluster and a triton cluster in relative $2s$-state motion.

[b]For the calculation of the ΔE's of these levels, we have used the cluster model wave functions described in reference 4 and in L. D. Pearlstein, Y. C. Tang, and K. Wildermuth, Nuclear Phys. 18, 23 (1960).

[c]Rotational level.

[d]For the distance of the outside nucleon from the center of the nucleus in the $(\frac{1}{2}+)$ state of N^{13} (C^{13}), we have assumed that it is the same as for the outside nucleon in the corresponding $(\frac{1}{2}+)$ level (0.871, 0.5 Mev) in F^{17} (O^{17}); the latter distance can be calculated from their Coulomb energy differences.

and O^{17} by the fact that the outside nucleon can be bound more strongly by a blown-up O^{16} cluster. In addition, one notes that here, one only needs one quantum of excitation rather than the two quanta of excitation needed to obtain the 6.06-Mev state in O^{16}. If we now estimate ΔE by this assumed structure, we indeed get a positive quantity in complete accord with the experimental situation. Furthermore, it was found[9] that this level in O^{17} does not exhibit stripping in the (d, p) reaction, thus further supporting our assumption about the structure of this level which we inferred from the study on the Coulomb energy behavior.

From the above discussion, we therefore conclude that by studying the sign and the order of magnitude of the excitation energy difference of mirror levels, valuable information can be obtained about the cluster structure of these levels. In some of the examples which we have mentioned, objections might be raised in that we have compared a bound state to a state in the continuum. Those examples are the comparisons of the mirror $(\frac{1}{2}-)$ state in O^{17} - F^{17} and the $(\frac{1}{2}+)$ levels in C^{13} - N^{13}. One might argue that since the nature of the external wave function describing clusters at large distances is quite different for a resonant state than for a bound state, any conclusion drawn from such comparisons might be rather doubtful. However, one must also note that for the decay of the $(\frac{1}{2}-)$ state in F^{17} and the $(\frac{1}{2}+)$ state in N^{13} the outside protons must penetrate through the Coulomb potential barrier; therefore, the wave function also decays exponentially in this region. Thus, in essence, those states behave very much as if they were indeed bound.

*Supported in part by Office of Naval Research.

[1]K. Wildermuth and Th. Kanellopoulos, Nuclear Phys. 7, 150 (1958); Nuclear Phys. 9, 449 (1958/59); CERN Report 59-23 (unpublished).

[2]G. C. Phillips and T. A. Tombrello (to be published).

[3]R. K. Sheline and K. Wildermuth, Bull. Am. Phys. Soc. 4, 271 (1960); B. Roth and K. Wildermuth, Bull. Am. Phys. Soc. 4, 271 (1960).

[4]W. E. Kunz, Phys. Rev. 97, 456 (1955); L. D. Pearlstein, Y. C. Tang, and K. Wildermuth, Phys. Rev. 120, 224 (1960).

[5]All the experimental data are taken from the compilation of F. Ajzenberg-Selove and T. Lauritsen, Nuclear Phys. 11, 1 (1959).

[6]Levels of the same rotational band means that these levels have the same cluster structure and the same order of relative oscillation of the clusters. For examples, the 0+, 2+, and 4+ states of Be^8 form a rotational band (see reference 1).

[7]U. Meyer-Berkhout, K. W. Ford, and A. E. S. Green, Ann. Phys. 8, 119 (1959).

[8]We thank Professor F. Ajzenberg for sending us the preprint in which this information is contained.

[9]T. S. Green and R. Middleton, Proc. Phys. Soc. (London) A69, 28 (1956).

OBSERVATION OF THE HYPERFINE STRUCTURE SPLITTING OF MUONIUM BY USE OF A STATIC MAGNETIC FIELD*

R. Prepost
Columbia University, New York, New York

and

V. W. Hughes and K. Ziock
Yale University, New Haven, Connecticut

(Received December 1, 1960)

The discovery of muonium through the observation of its characteristic Larmor precession frequency[1] may make possible a precision measurement of the hyperfine structure interval $\Delta\nu$ in the ground $1\,^2S_{1/2}$ state of muonium in a microwave experiment. As a preliminary to such an experiment in order to obtain a rough measurement of $\Delta\nu$ and to confirm further the expected behavior of muonium, the effect of a static magnetic field on the polarization of muons has been studied. The type of experiment described here has already been done for muons stopping in solids.[2]

The principle of the experiment can be understood by considering the Breit-Rabi energy level diagram[3] of the ground state of muonium. The direction of the applied static magnetic field H, which is also the direction of the axis of quantization, is taken along the direction of the incoming muon beam. If muonium is formed by a polarized

muon capturing an electron from a gas atom at weak magnetic field, the hyperfine structure magnetic substates $(F, m_F) = (1,-1)$, $(1,0)$, $(0,0)$, and $(1,+1)$ will be populated in the relative amounts 1/2, 1/4, 1/4, and 0, respectively, where F is the quantum number for total atomic angular momentum and m_F is the associated magnetic quantum number.[4] In the substates $(1,0)$ and $(0,0)$ the muon is unpolarized, whereas in the substate $(1,-1)$ it retains its initial polarization. If muonium is formed at strong magnetic field, where the magnetic quantum numbers m_μ and m_J for the muon and electron are good quantum numbers, then the magnetic substates $(m_\mu, m_J) = (-1/2,-1/2)$, $(-1/2,+1/2)$, $(+1/2,+1/2)$, and $(+1/2,-1/2)$ will be populated in the relative amounts 1/2, 1/2, 0, and 0, and hence the muon will retain its initial polarization. The angular distribution of the decay positrons is related to the muon spin direction by the proportionality

$$N_{e^+}(\theta)\, d\Omega \propto (1 + PA\, \cos\theta) d\Omega, \qquad (1)$$

where P is the muon polarization, A is the asymmetry parameter, and θ is the angle between the directions of the muon spin and of the positron emission.[5] Specifically, the resultant polarization for muons forming muonium depends on the values of the magnetic field and of the hyperfine structure separation $\Delta\nu$ according to the equation

$$P = \tfrac{1}{2} + \tfrac{1}{2}\left(\frac{x^2}{1+x^2}\right), \qquad (2)$$

where $x = (g_J - g_\mu)\mu_0 H/\Delta W$, and g_J = electron g value ($\simeq +2$); g_μ = muon g value; μ_0 = electron Bohr magneton; ΔW = hyperfine structure splitting ($\Delta W/h = \Delta\nu = 4500$ Mc/sec); H = external magnetic field. Equations (1) and (2) indicate that $\Delta\nu$ can be measured in principle by observing the number of positron counts as a function of the magnetic field H.

The experimental arrangement is shown in Fig. 1. The counter array consists of five counters placed in an external meson beam of the Nevis synchrocyclotron. A large solenoid provides a longitudinal magnetic field. The target is a stainless steel tank containing purified argon gas at a pressure of 55 atmospheres, and sufficient absorber is placed between counters 1 and 2 so that only muons stop in the gas target. A stopped muon is signified by a $12\bar{3}$ coincidence and a decay positron by a $34\bar{2}$ coincidence. De-

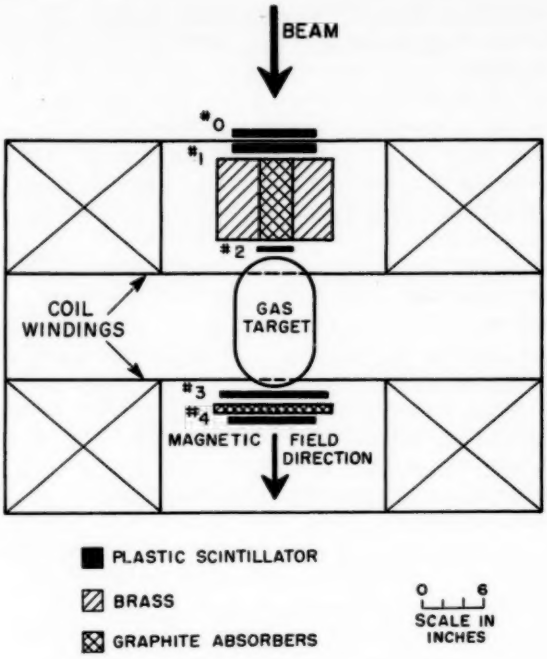

FIG. 1. Experimental arrangement.

cay positrons are counted from 0.2 μsec to 3.2 μsec after a muon enters the target, and the positron counts are recorded as a function of the magnetic field which is varied from 100 to 5800 gauss. Since the magnetic field influences the trajectories of the charged particles, it was necessary to obtain data with a dummy target consisting of an identical stainless steel tank containing aluminum sheets and having equivalent stopping power and geometry to the gas target. Effects due to muonium formation could then be distinguished since it is known that muons are not depolarized in aluminum.

The results of the experiment are shown in Fig. 2. The quantity R is the ratio of the positron counting rate for the dummy target to the positron counting rate for the gas target with both rates normalized to 1 at $H = 0$. The data points are indicated together with their error bars which represent plus or minus one standard deviation. The solid curve is the theoretical curve which corresponds to the expected theoretical value of $\Delta\nu = 4500$ Mc/sec, whereas the two dashed curves correspond to $\Delta\nu = 2250$ Mc/sec and $\Delta\nu = 9000$ Mc/sec. The theoretical curves are drawn on the assumption that all the muons stopped in the argon gas form muonium, which is supported

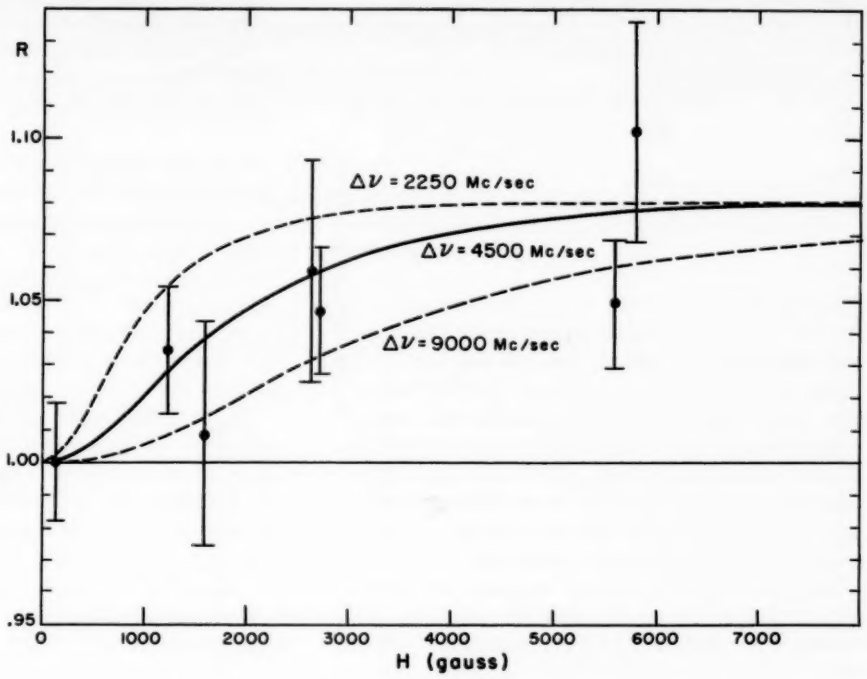

FIG. 2. Experimental data and theoretical curves for the quantity R versus the magnetic field H.

by evidence from the earlier experiment.[1] The data are consistent with the assumptions that $\Delta\nu = 4500$ Mc/sec and that all the muons form muonium, and indeed indicate that $\Delta\nu$ lies between 2250 Mc/sec and 9000 Mc/sec.

*This research was supported in part by the Air Force Office of Scientific Research (with Yale) and also by the Office of Naval Research and the U. S. Atomic Energy Commission (with Columbia).

[1]V. W. Hughes, D. W. McColm, K. Ziock, and R. Prepost, Phys. Rev. Letters 5, 63 (1960).

[2]For a summary on this type of experiment, see G. R. Lynch, J. Orear, and S. Rosendorff, Phys. Rev. 118, 284 (1960).

[3]P. Kusch and V. W. Hughes, Encyclopedia of Physics, edited by S. Flügge (Springer-Verlag, Berlin, 1959), Vol. 37, Part 1, p. 90.

[4]G. Breit and V. W. Hughes, Phys. Rev. 106, 1293 (1957).

[5]R. L. Garwin, L. M. Lederman, and M. Weinrich, Phys. Rev. 105, 1415 (1957).

OBSERVATIONS OF EXTENSIVE AIR SHOWERS NEAR THE MAXIMUM OF THEIR LONGITUDINAL DEVELOPMENT*

J. Hersil and I. Escobar
Laboratorio de Fisica Cosmica, Universidad Mayor de San Andres, La Paz, Bolivia

and

D. Scott, G. Clark, and S. Olbert
Laboratory for Nuclear Science, Massachusetts Institute of Technology, Cambridge, Massachusetts
(Received November 28, 1960)

Extensive air showers have been studied at an altitude of 4200 m (atmospheric depth 630 g/cm^2) with apparatus previously used at sea level.[1-3] Their characteristics are found to differ markedly from those of showers at sea level, and demonstrate that vertical showers with about 30×10^6 particles are near their maximum development. These results were derived from data on approximately 400 selected showers with sizes greater than 15×10^6 particles.

The experimental method[2] employs the techniques of fast-timing and density sampling with eleven 1-m^2 scintillation detectors in an array with outside diameter 700 m. The apparatus is located on the Altiplano at El Alto near La Paz, Bolivia. For each shower event the arrival direction is determined from the timing data to within 5°. The size and core location are determined by a least-squares fitting of the density data to a trial function representing the lateral distribution. Tests of the analysis procedure on artificial shower data generated by a Monte Carlo method demonstrate that the average error displacement in the core location is about 10 m, and that the fractional error in the size determination is about 8%, provided the trial function is an accurate representation of the lateral distribution. The function used throughout the analysis was the Greisen representation[4] of the Nishimura-Kamata function (NKG) with the age parameter $s = 1.0$ and the Molière unit equal to 132 m.

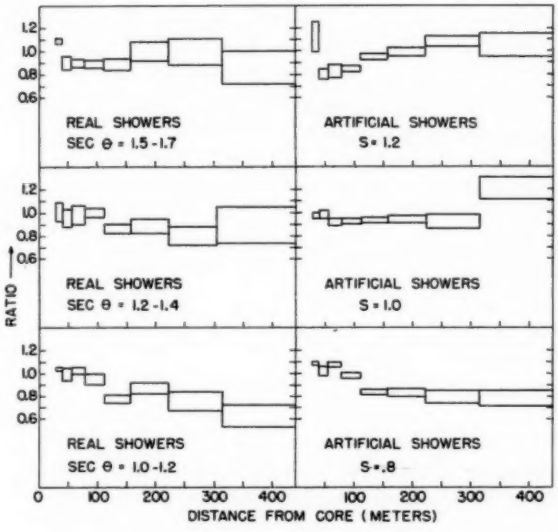

FIG. 1. Comparison of the observed lateral distributions with the trial function NKG 1.0 for three groups of real events with sizes from 18×10^6 to 25×10^6, and for three groups of artificial events. The abscissa represents the distance from the calculated core position. The ordinate represents the ratio between the average observed particle density and the average density calculated according to the fitted trial function. The height of each box indicates the statistical and instrumental uncertainty.

We first compared the observed average lateral distributions with the trial function, for showers grouped according to their sizes and zenith angles. A part of these results for one size group (18×10^6-25×10^6) are shown in Fig. 1, where the ratios of the observed particle densities to the densities calculated from the fitted trial function are plotted versus the distance from the core. Also plotted are the ratios found for artificial shower data generated using the NKG function with values of s equal to 0.8, 1.0, and 1.2. The results for artificial showers indicate that the method of analysis can reveal a systematic trend in the steepness of the lateral distribution. The results for real showers therefore support the conclusion that the steepness of the lateral distribution decreases with zenith angle. (By comparison, at sea level the lateral distribution shows little or no variation with zenith angle and can be fitted by the NKG function for $s = 1.3$).[3] Note that our results are essentially limited to core distances from about 40 m to 400 m.

We then plotted the integral intensity S of showers with sizes greater than N as a function of

$\sec\theta$. We selected events according to criteria which permitted accurate evaluation of the detection efficiency. The calculated sizes were corrected for errors caused by the systematic change with θ in the lateral distribution function as discussed previously.

Whereas, at sea level, S for fixed N can be expressed as an exponential function of $\sec\theta$ (which is proportional to the slant thickness of the atmosphere), at 4200 m we find that S (for N near 30×10^6) is approximately stationary with respect to changes in $\sec\theta$ near $\sec\theta = 1.0$. This is the behavior expected if showers with $N \approx 30\times10^6$ are near their maximum longitudinal development.

The same data can be used to determine directly the longitudinal development. For this purpose we plotted S versus N for events grouped according to zenith angle. For each group we evaluated the average slant thickness of the atmosphere, $x = x_0 \sec\theta$, where $x_0 = 630$ g/cm^2. We then read from these plots the values of N at several given values of S. In this way we obtained the data on the variation of N with x at constant S which are shown in Fig. 2. If the primary flux is isotropic, and if there were no fluctuations in shower development, then each set of points in Fig. 2 would represent the dependence of size on depth for showers initiated by primaries of a certain specific energy. Even with fluctuations present, Fig. 2 should indicate the general features of the dependence on $\sec\theta$ of the average size of showers initiated by primaries of a given energy. We wish to emphasize that the important feature of these curves is the presence of the maximum near 630 g/cm^2.

Also shown in Fig. 2 is the analogous result from the earlier sea level experiment[3] on the variation of N with x at one of the same absolute values of S. The discrepancy in size at equivalent atmospheric depth is not yet understood.

A more complete report on this work including results on showers with sizes less than 10^7 particles is in preparation.

The authors express their thanks to R. Schulczewski, who has assisted in the operation of the experiment, and to the Massachusetts Institute of Technology Computation Center for the use of the IBM-704 computer.

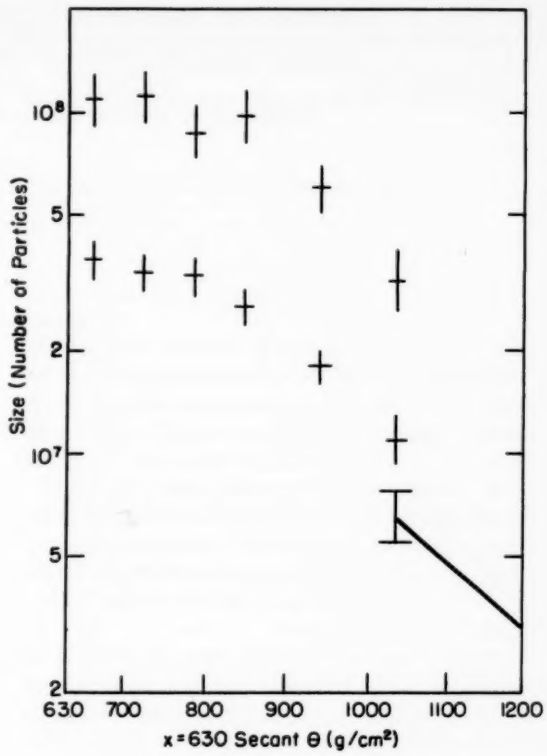

FIG. 2. Experimental results on the longitudinal development of extensive air showers. The plot is derived from the observed integral size spectra at various zenith angles and represents the dependence of N on x at constant S. The upper and lower sets of points are for $S = 10^{-14}$ cm^{-2} sec^{-1} sr^{-1} and $S = 10^{-13}$ cm^{-2} sec^{-1} sr^{-1}, respectively. The straight line with an error indicator represents the analogous results derived from sea level data for $S = 10^{-13}$ cm^{-2} sec^{-1} sr^{-1}.

*This work is supported in part through a contract with the U. S. Air Force, in part by funds provided by the U. S. Atomic Energy Commission, the Office of Naval Research, and in part by the Massachusetts Institute of Technology Computation Center.

[1]G. Clark, J. Earl, W. Kraushaar, J. Linsley, and F. Scherb, Nature 180, 353 (1957).

[2]G. Clark, J. Earl, W. Kraushaar, J. Linsley, B. Rossi, and F. Scherb, Suppl. Nuovo cimento 8, 623 (1958).

[3]B. Rossi, Proceedings of the Moscow Cosmic-Ray Conference (Moscow, 1960), Vol. II, p. 18.

[4]K. Greisen, Progress in Cosmic-Ray Physics (North Holland Publishing Company, Amsterdam, 1956), Vol. IV, Chap. 1.

ASYMMETRY PARAMETER OF Λ DECAY AND THE INTERMEDIATE BOSON OF WEAK INTERACTIONS*

S. Oneda
Department of Physics, Kanazawa University, Kanazawa, Japan

J. C. Pati†
Department of Physics, California Institute of Technology, Pasadena, California

and

B. Sakita
Department of Physics, University of Wisconsin, Madison, Wisconsin

(Received November 28, 1960)

The magnitude of the pion asymmetry parameter α^- of the $\Lambda \to p + \pi^-$ decay has been determined[1] to be greater than or equal to (0.73 ± 0.14). The sign of this parameter, however, is rather hard to find. The results of Boldt et al.[2] and the preliminary results of Birge and Fowler[3] indicated a positive sign for α^-. Recently, however, Birge and Fowler[4] have reported a negative sign for α^-, contrary to their own preliminary[3] results.

In this Letter we wish to point out that the negative sign of α^-, provides a favorable argument for the conjecture that the V-A four-fermion interaction may be mediated by a vector boson.

A related problem has already been discussed in our previous work,[5] which is referred to as I in the Letter. There, however, we have developed the arguments under the assumption that the sign of α^- is positive, which was believed to be true at that time. The purpose of this note is to stress the implications of the negative sign. Let us adopt,[6] as in I, more or less in the spirit of the Sakata model, the tetrahedron scheme of four-fermion interactions, mediated by the charged vector bosons $B^{\pm}$. The weak interaction is thus assumed to be

$$H_{\text{weak}} = J_\alpha B_\alpha + \text{H.c.}, \qquad (1)$$

where[7]

$$J_\alpha = F[\bar{e}\gamma_\alpha(1+\gamma_5)\nu + \bar{\mu}\gamma_\alpha(1+\gamma_5)\omega + \bar{n}\gamma_\alpha(1+\gamma_5)p + (F'/F)\bar{\Lambda}\gamma_\alpha(1+\gamma_5)p]. \qquad (2)$$

The results of the local four-fermion interaction are obtained by taking the limit $m_B \to \infty$ and $F^2/m_B{}^2 \to G/\sqrt{2}$, where G denotes the usual Fermi coupling constant and m_B, the mass of the vector boson.

Starting with the above interaction, it was indicated in I that Fig. 1(b) may be the dominant diagram for $\Lambda \to N + \pi$ decays, instead of Fig. 1(a) (which had previously been considered[8] as the dominant diagram) for the following four reasons.

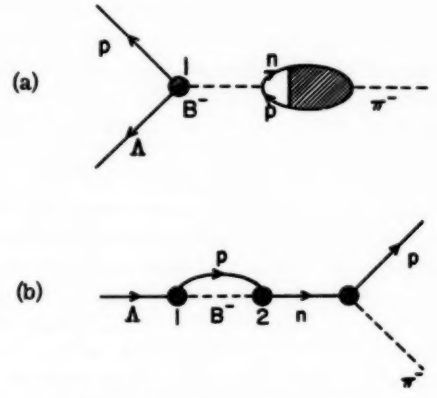

FIG. 1. Typical diagrams for $\Lambda \to p + \pi^-$ decay.

(i) From the point of view of dispersion relation calculations, taking the mass of Λ as a variable of the dispersion integral, the single-neutron state [Fig. 1(b)] is the lowest mass intermediate state contributing to the imaginary part of the matrix element.

(ii) While Fig. 1(a) contains an appreciable amount of $|\Delta\vec{I}| = 3/2$ transitions, Fig. 1(b) satisfies the strict $|\Delta\vec{I}| = \frac{1}{2}$ rule. Thus the dominance of Fig. 1(b) may be at the root of the approximate validity of the $|\Delta\vec{I}| = \frac{1}{2}$ rule.

(iii) If Fig. 1(a) is the main mechanism of $\Lambda \to N + \pi$ decays, it can explain the observed rate of Λ decay for a choice of $F' \approx (2.5)^{1/2} F$, while the slow leptonic modes of Λ and K-meson decays seem to require $F' \approx F/(10)^{1/2}$. If, however, Fig. 1(b) dominates over Fig. 1(a) [say, by a factor $\approx (20)^{1/2}$ in the matrix elements], one can hope to explain the rates of both leptonic and nonleptonic modes of strange particle decays with a single choice of F' [i.e., $F' \approx F/(10)^{1/2}$].

(iv) An actual perturbation-theoretic calculation[9] reveals the following:

(a) For reasonably finite values of m_B ($m_K < m_B < 2m_p$, say), the contribution of Fig. 1(b) is considerably bigger than that of Fig. 1(a).[10] For instance, one obtains [without any renormalization effects at vertices 1 and 2 in Fig. 1(b)] the following values for the absolute square of the ratio of the matrix elements:

$$|M[\text{Fig. 1(b)}]/M[\text{Fig. 1(a)}]|^2 \approx 8.8 \text{ for } \lambda \approx m_\Lambda,\ m_B \approx m_p,$$
$$\approx 73.6 \text{ for } \lambda \approx 1.5 m_p,\ m_B \approx m_p, \quad (3)$$

where λ denotes the Feynman cutoff parameter introduced to evaluate M [Fig. 1(b)].

(b) In the local limit ($m_B \to \infty$), the contribution of Fig. 1(b) vanishes for bare V-A interaction. However, as shown in I, introduction of renormalization effects[11] at vertices 1 and 2 leads to significant contribution from Fig. 1(b). The introduction of such effects for finite values of m_B does not alter the qualitative aspects of the situation mentioned above in (a).

Thus we will proceed by assuming[12] that Fig. 1(b) is indeed the dominant diagram for Λ decay, even compared to diagrams other than Fig. 1(a). An important fact to be noticed now is the sign of the asymmetry parameter α^- given by Fig. 1(b), as a function of m_B. The following remarks are pertinent in this connection.

(1) Introducing the renormalization effects at vertices 1 and 2, as mentioned in reference 11, the matrix elements of Figs. 1(a) and 1(b) are found[9] to be proportional to

$$M[\text{Fig. 1(a)}] \propto \bar{u}_p(\gamma \cdot p_\pi)(1 + A\gamma_5)u_\Lambda, \quad (4)$$

$$M[\text{Fig. 1(b)}] \propto \bar{u}_p(\gamma \cdot p_\pi)(\alpha + \beta\gamma_5)u_\Lambda, \quad (5)$$

where

$$\alpha = (A - B)O_1 - (A + B)(m_\Lambda/m_p)O_2,$$
$$\beta = (1 - AB)O_1 + (1 + AB)(m_\Lambda/m_p)O_2. \quad (6)$$

O_1 and O_2 are known[9] functions of m_Λ, m_p, m_B, and the cutoff parameter λ. The variations of O_1 and O_2 as a function of m_B are given in Table I for $\lambda = m_\Lambda$. The same qualitative behavior is obtained for other choices of λ.

(2) For positive values of A,[13] it is clear from Eq. (4) that Fig. 1(a) leads to a positive[14] sign for α^-, independent of the value of m_B.

(3) For finite values of m_B, and with no renormalization effects at vertices 1 and 2 in Fig. 1(b) (i.e., with $A = B = +1$), it is clear from Eq. (6) that $\beta/\alpha = -1$ for all values of the cutoff λ. This leads to negative values of the asymmetry parameter α^-.

(4) The above conclusion regarding the sign of α^- holds, even if we introduce renormalization effects at vertices 1 and 2, as long as A and B are positive. Thus the conclusion for finite values of m_B is not so sensitive to the choice of the renormalization effects.

(5) In the local limit ($m_B \to \infty$), $O_2 \to 0$ (see Table I). In this case the conclusion depends rather strongly on the choice of the renormalization effects, since without any renormalization effect, i.e., for $A = B = +1$, α and $\beta \to 0$ as $m_B \to \infty$. For a choice of A and $B > 1$, with $B > A$, however, α^- is positive (see Table I, last column).

Thus we find that the negative sign of α^- may

Table I. Asymmetry parameter of $\Lambda \to p + \pi^-$ decay.[a]

m_B (Mev)	$O_1 \times 10^2$	$O_2 \times 10^2$	α^- ($A = B = +1$)	α^- ($A = +1$, $B = +1.25$)
500	4.29	-5.71	-0.90	-0.948
938	5.55	-5.20	-0.90	-0.95
1876	7.43	-4.05	-0.90	-1.0
4690	17.40	-1.09	-0.90	+0.573
∞	40.48	0	Zero amplitude	+0.90

[a]The values listed in this table are for a choice of the cutoff $\lambda = m_\Lambda$. Column 4 gives the asymmetry parameter α^- for Fig. 1(b) without any renormalization effect at vertices 1 and 2 ($A = B = +1$). Column 5 gives α^- for a particular choice of the renormalization effects ($A = +1$, $B = +1.25$).

indeed favor the intermediate-boson hypothesis. Since we have little knowledge of the true nature of the renomalization effects at vertices 1 and 2, we cannot, however, conclude that the negative sign of α^- would totally exclude the local four-fermion interaction, while the positive sign would exclude the nonlocal one. The purpose of this Letter is, however, to stress that, if future experiments confirm a negative sign for α^-, there is a more straightforward way to understand this result simply (even without any renormalization effects) within the intermediate-boson framework (m_B finite) than without it ($m_B \to \infty$). On the other hand, if experiments confirm a positive sign for α^-, the same picture will favor a local four-fermion interaction rather than a nonlocal one.

With our present experimental limitations, we have to infer the existence of the B meson from processes where its role as a virtual intermediate particle may be important. In this connection, it is important to recall that the introduction of a B meson with mass nearly equal to the mass of the K meson gives rise to a nonlocal effect,[15] which could explain[16] the observed lifetimes of O^{14} and μ decay on the hypotheses of strictly universal couplings and conserved vector current.[17] It also accounts for the recently observed[18] value of the Michel parameter, $\rho = 0.78 \pm 0.025$, which is slightly higher than the normally expected value 0.75. The implication[19] from the slowness of $\mu \to e + \gamma$ decay is an unsettled[16] question, until one determines[20] the nature of the neutrinos associated with the muon and the electron. On the basis of the picture presented in this Letter, the sign of the asymmetry parameter α^- could favor or disfavor the intermediate-boson hypothesis.

Two of us (S. O. and J. C. P.) would like to thank Professor John S. Toll for the extremely kind hospitality extended to them during their stay at the University of Maryland, where part of this work was carried out. One of us (J. C. P.) takes pleasure in thanking Professor M. Gell-Mann for his critical comments, and the California Institute of Technology for the offer of the Richard C. Tolman Fellowship.

---

*This research was supported in part by the U. S. Air Force through the Air Force Office of Scientific Research of the Air Research and Development Command. Supported in part by the University of Wisconsin Research Committee with funds granted by the Wisconsin Alumni Research Foundation and in part by the U. S. Atomic Energy Commission.

†Richard C. Tolman Postdoctoral Fellow.

[1]D. A. Glaser, report at the Ninth Annual International Conference on High-Energy Physics, Kiev, 1959 (unpublished).

[2]E. Boldt, H. S. Birge, D. O. Caldwell, and Y. Pal, Phys. Rev. Letters 1, 256 (1958).

[3]R. W. Birge and W. B. Fowler, Bull. Am. Phys. Soc. 4, 355 (1959).

[4]R. W. Birge and W. B. Fowler, Phys. Rev. Letters 5, 254 (1960).

[5]S. Oneda, J. C. Pati, and B. Sakita, Phys. Rev. 119, 482 (1960). Other references are cited here.

[6]The extension of our arguments to other intermediate-boson models, such as proposed by T. D. Lee and C. N. Yang, Phys. Rev. 119, 1410 (1960), is straightforward and leads to similar conclusions to those discussed here.

[7]It is pertinent to notice that the arguments in this Letter will rest heavily on the belief that all currents in J_α, including the (Λp) current, have the same chiral form, i.e., positive chiral form as in β decay.

[8]See for instance, S. Okubo, R. E. Marshak, and E. C. G. Sudarshan, Phys. Rev. 113, 944 (1959).

[9]See reference 5. For details, see J. C. Pati, thesis, University of Maryland, 1960, Physics Department Technical Report No. 193 (unpublished).

[10]The contribution of Fig. 1(a) is calculated from the observed rate of $\pi \to \mu + \nu$ decay.

[11]This was done phenomenologically in I by replacing vertices 1 and 2 in Fig. 1(b) by $f'\gamma_\alpha(1 + A\gamma_5)$ and $f\gamma_\alpha(1 + B\gamma_5)$, respectively. A and B denote the renormalization effects and were treated as positive constants. For the purpose of orientation, we had adopted $A \approx 1$, $B \approx +1.25$. The exact choice of A and B, however, does not affect our arguments in the present Letter regarding the sign of α^- for finite values of m_B, as long as A and B are considered as positive.

[12]The application of such a picture to K-meson decays seems to be consistent with the relative rates of all the decay modes of the K meson. See J. C. Pati, S. Oneda, and B. Sakita, Nuclear Phys. 18, 318 (1960).

[13]Starting from bare positive chiral currents, it is reasonable to assume that the strong virtual effects are perhaps not so drastic as to lead to negative values for either A or B or both.

[14]Thus, if α^- turns out to be negative, Fig. 1(a) can clearly be excluded from being the dominant mechanism of Λ decay.

[15]T. D. Lee and C. N. Yang, Phys. Rev. 108, 1611 (1957).

[16]S. Oneda and J. C. Pati, Phys. Rev. Letters 2, 516 (1959).

[17]R. P. Feynman and M. Gell-Mann, Phys. Rev. 109, 193 (1958).

[18]R. J. Plano, Phys. Rev. 119, 1400 (1960). The value quoted includes electromagnetic corrections.

[19]G. Feinberg, Phys. Rev. 110, 1482 (1958); P. Meyer and G. Salzman, Nuovo cimento 14, 1310 (1959).

[20]T. D. Lee and C. N. Yang, Phys. Rev. Letters 4, 307 (1960); B. Pontecorvo, Soviet Phys.–JETP 10(37), 1751 (1959).

TEST FOR K^--HYPERON RELATIVE PARITY

B. A. Jacobsohn* and R. M. Ryndin†
CERN, Geneva, Switzerland
(Received December 13, 1960)

Numerous experiments which could determine the (K^-, Λ) or (K^-, Σ) relative parities have been suggested in the last several years. In addition to examinations of threshold behaviors, they include experiments with K in flight,[1] reactions on polarized targets,[2] with polarized beams,[1,3] and those in which the hyperon emerges in a hyperfragment.[4] In the latter case, the spin and orbital parity of the fragment present additional unknown quantities.

We wish to discuss here a parity test with stopped K^- utilizing an unpolarized target. To the best of our knowledge, one such test (K^- on d) has been suggested in the literature[5]; however, it requires the assumption that the meson be absorbed predominantly from an s state. A series of papers[6] has recently appeared giving theoretical discussions in support of this assumption. The arguments leading to the conclusion of pure s absorption involve the strong mixing of the s states into the high-l states through the Stark effect produced by fields of neighboring atoms. It is sufficiently difficult to come to a reliable quantitative conclusion regarding the fraction of p-state capture that we believe that it is useful to present arguments which show that the same kind of experiment suggested by Sirlin and Spitzer,[5] when applied to He, yields a parity test which is independent of any special assumptions about the K absorption, except of course that it should conserve parity and that the K have zero spin. In this connection, it should been remarked that the dominance of s over p capture is expected to be less in (K, He) than in (K, d).

Since the result has implications for a variety of processes, we prefer to give the discussion in general terms. Consider in the c.m. frame a reaction $K^- + \mathrm{He}^4 \rightarrow$ any number of particles, all with relative momenta which are parallel or antiparallel in a direction which we call $\vec{k}$, and take parallel to z. Of course, for the K and α one can substitute any two spin-zero particles. The particles in the final state have intrinsic angular momenta which can add up to the total spin values $S, S', \cdots$. We decompose the initial wave function into orbital angular momentum states $|lm_l\rangle$, but make no assumption here about the relative amplitudes of the latter. The discussion can therefore be applied to initial plane waves as well as to bound states.

Under a reflection R in the x-z plane (inversion followed by 180° rotation about the y axis) the final state and the initial components transform, respectively, as

$$R|\vec{k}Sm_S\rangle = (-1)^{S-m_S}\mathcal{P}_f|\vec{k}S-m_S\rangle,$$

$$R|lm_l\rangle = (-1)^{l-m_l}(-1)^l\mathcal{P}_i|l-m_l\rangle, \qquad (1)$$

in which $\mathcal{P}_{f,i}$ represent the products of all intrinsic parities in the final and initial states. Next we make use of the fact that the final-state plane wave contributes no z component of orbital angular momentum; it is at this point in the argument that, in the case of three outgoing particles, we require that the directions of the final momenta coincide. Then angular momentum conservation gives $m_l = m_S \equiv m$. The invariance of the S matrix gives in turn

$$\langle\vec{k}Sm|S|lm\rangle = \mathcal{P}_i\mathcal{P}_f(-1)^S\langle\vec{k}S-m|S|l-m\rangle. \qquad (2)$$

The result which we shall use follows immediately from Eq. (2):

$$\mathcal{P}_i\mathcal{P}_f(-1)^S = -1 \text{ forbids } m = 0. \qquad (3)$$

The experimental implications of this statement must be examined separately in each case. The simplest one, that in which all final particles have zero spin, makes the process completely forbidden if $\mathcal{P}_i\mathcal{P}_f = -1$, in agreement with the result of Bohr.[1] Bohr's symmetry operation can make a stronger statement about this process than does ours, since he can forbid three-particle final states with two arbitrary momentum directions provided that the initial K is in flight in the same plane. His conservation law and relation (3) have a large area of overlap, but they are not identical in content since we have invoked rotational invariance about the z axis in addition to the reflection R.

For the K^--hyperon parity test, we consider states in which two of the final particles have spin $\frac{1}{2}$ and in which all final-state momenta are

parallel:

$$K^- + \mathrm{He}^4 \to \begin{Bmatrix} \mathrm{H}^3 \\ \mathrm{He}^3 \end{Bmatrix} + \begin{Bmatrix} \Lambda \\ \Sigma \end{Bmatrix} + n\pi. \quad (4)$$

A specification of the precise nature of the initial state can still be deferred; we denote it by ψ. We now show that a measurement of the sign of the spin correlation averaged over all directions perpendicular to $\vec{k}$ gives a direct determination of $\mathcal{P}_i\mathcal{P}_f$. Indeed, the operator

$$C_\perp \equiv \tfrac{1}{2}(\sigma_x{}^1\sigma_x{}^2 + \sigma_y{}^1\sigma_y{}^2) = \tfrac{1}{2}(\vec{\sigma}^1\cdot\vec{\sigma}^2 - \sigma_z{}^1\sigma_z{}^2) \quad (5)$$

is diagonal in S and m. The triplet $m=\pm1$ states contribute zero to $\langle C_\perp\rangle$; the triplet and singlet $m=0$ states contribute +1 and -1, respectively. Combining this with relation (3), we find the final result

$$\langle C_\perp\rangle = -A_{00}(A_{00}+A_{11}+A_{1-1})^{-1}, \quad \mathcal{P}_i\mathcal{P}_f = +1, \quad (6a)$$

$$= +A_{10}(A_{10}+A_{11}+A_{1-1})^{-1}, \quad \mathcal{P}_i\mathcal{P}_f = -1, \quad (6b)$$

in which $A_{Sm} \equiv |\langle \vec{k}Sm\,|\,\mathcal{S}\,|\,\psi\rangle|^2$ and can include contributions from all l.

It is clear that $\langle C_\perp\rangle$ can be replaced by $\langle C_y\rangle$ if the absorption is from a mesonic atom which has lost all directional memory of its formation process.

The processes (4) in which no pions emerge have very small branching ratios. When one pion is emitted, it is important to estimate how large an angle θ can be tolerated before condition (6) breaks down, where θ is the c.m. angle between the two momenta which are taken to lie in the x-z plane. To do this, we note that the pion will have momentum $\sim(1\text{ to }2)\mu c$. If we assume an interaction radius $\sim\hbar/\mu c$ for (4), pion d waves at the highest will be involved and it is unlikely that $\langle C_\perp\rangle$ or $\langle C_y\rangle$ will change sign when $\theta \lesssim \pi/4$. Furthermore, pure s-wave absorption of the K would give $\langle C_y\rangle = \mp 1$ ($\mathcal{P}_i\mathcal{P}_f = \pm 1$) for <u>arbitrary</u> θ. This latter result comes from the Bohr operation, according to which one applies the operator R to initial and final state, but with all spins quantized along y. (It is straightforward to show that $\langle C_\perp\rangle$ also carries the unique sign in the s-capture case, but there is no restriction on its absolute value.) Since we can reasonably expect at least a large part of the capture to be from s states, a combination of the above two estimates makes it appear likely that the correlation $\langle C_\perp\rangle$ or $\langle C_y\rangle$ resulting from an unpolarized K-mesonic atom will not change sign as θ ranges through all values. A quantitative measurement of $\langle C_y\rangle$ could give a direct indication of the fraction of the absorption arising from states with $l>0$,

To know $\langle C\rangle$, one must have simultaneous information on the polarization directions of the nucleus and the hyperon. In special cases knowledge of the individual polarizations can be shown to yield the sign of $\langle C_y\rangle$; the extreme case in which $P_1, P_2 = \pm 1$ is obvious. If the strange particle is a Λ or Σ^+, its own decay would serve as the polarization signature once the sign of the asymmetry parameter α is settled.[7] The Σ^0 polarization could also be inferred from that of the daughter Λ using the well-known parity-independent relation[8] $\langle P_\Lambda\rangle = -\frac{1}{3}P_{\Sigma^0}$. The nuclear spin direction affects the right-left asymmetry of the elastic scattering of the recoil nucleus (which has $E_{\max}\sim 50$ Mev, but $\langle E\rangle$ probably much lower) on He, or the asymmetry in a stripping reaction such as $\mathrm{He}^3(\alpha,p)\mathrm{Li}^6$. The dependence of these processes on polarization is apparently not yet known.

We next relate the above discussion to the (K^-,d) atom. It is clear that the preceding arguments rest on the complete correlation between parity and initial angular momentum in Eq. (2); i.e., $l=j$. For the spin-one deuteron this correlation is lost and the general argument no longer holds. If, however, one assumes all processes to come from the s state so that the initial state is pure 1^+, the correlation is regained. One has again relation (3) and Eqs. (6), all with a change of sign, in agreement with the Sirlin-Spitzer result[5] when no pions emerge. In the case of pion emission the same argument can be applied if the momenta are parallel, whatever might be the relative orbital angular momentum of the baryons.

We conclude with two examples of other uses of relation (3). The first concerns the reaction

$$K^- + \mathrm{He}^4 \to {}_\Lambda\mathrm{H}^4 + \pi^0; \quad (7a)$$

$${}_\Lambda\mathrm{H}^4 \to \mathrm{He}^4 + \pi^-. \quad (7b)$$

The angular distribution for the products of (7b) when $j=1$ has been discussed by Dalitz and Downs[4] using Clebsch-Gordan analysis. For $\mathcal{P}_\pi\mathcal{P}_K\mathcal{P}_{\mathrm{Frag}} = +1$, they show that a certain Clebsch-Gordan coefficient vanishes and that therefore the $m=0$ state is absent, giving rise to a pure $\sin^2\theta$ distribution. The same result is seen immediately from (3).

Secondly, the relation has a low-energy nuclear physics application as a detector of nuclear alignment. Consider $X(d,\alpha)Y^*$ in which X and Y^* are both 0^+ states. Then, choosing the line of flight

of the deuteron as the z axis, we see that (3) completely forbids the process to proceed from the $m=0$ state for all scattering angles. If this reaction is used to analyze the deuterons coming from some primary reaction, it can serve as a sensitive detector of the angular dependence of $\langle T_{20}\rangle \sim \langle 3S_z^2 - 2\rangle$.

Although reactions of the above type to low-lying levels of light nuclei are forbidden by isotopic spin conservation, one can break the T selection rule by choosing sufficiently heavy nuclei. An example[9] is the exothermic reaction $Si^{28}(d,\alpha)Al^{26*}$ to the first excited state of Al^{26}.

The authors are indebted to Professor L. Madansky for several stimulating and helpful discussions, and are grateful to CERN for its hospitality.

*Present address: University of Washington, Seattle, Washington.

†Permanent address: Joint Institute for Nuclear Research, Dubna, U.S.S.R.

[1]A. Bohr, Nuclear Phys. 10, 486 (1959).

[2]S. M. Bilenky, Nuovo cimento 10, 1049 (1958).

[3]S. M. Bilenky and R. M. Ryndin, Nuovo cimento 12, 106 (1959).

[4]R. H. Dalitz and B. W. Downs, Phys. Rev. 111, 967 (1958).

[5]A. Sirlin and R. Spitzer, Phys. Rev. Letters 3, 110 (1959).

[6]Summarized by G. A. Snow, Proceedings of the Tenth Annual Rochester Conference on High-Energy Nuclear Physics (to be published), Session S III, 41; a complete list of references is given there.

[7]R. W. Birge and W. B. Fowler, Phys. Rev. Letters 5, 254 (1960).

[8]R. Gatto, Phys. Rev. 109, 610 (1958); G. Feldman and T. Fulton, Nuclear Phys. 8, 106 (1958).

[9]C. P. Browne, Phys. Rev. 114, 807 (1959).

$N\bar{N} \leftrightarrow \pi\pi$ AMPLITUDE AND THE ELECTROMAGNETIC STRUCTURE OF THE NUCLEON*

James S. Ball† and David Y. Wong†
University of California, La Jolla, California
(Received November 14, 1960)

Recently, the effect of a pion-pion P-wave resonance on the $N\bar{N}$ to $\pi\pi$ amplitude and the electromagnetic structure of the nucleon has been investigated by Frazer and Fulco.[1] Their calculation suffers from two deficiencies: (1) The "rescattering cut" they employed produces divergent integrals which necessitate a cutoff. (2) Their "one-pole" effective-range formula corresponds to an extremely short-range pion-pion force and is inconsistent with the crossing symmetry of the pion-pion problem.[2]

The purpose of this Letter is to remedy both of these difficulties. (1) By crossing symmetry, the $N\bar{N}$ to $\pi\pi$ amplitude at zero total energy is identical to the forward pion-nucleon scattering amplitude, which can be calculated directly from experimental information. Having thus determined the $N\bar{N}$ to $\pi\pi$ amplitude at one point, one can calculate both this amplitude and the nucleon form factors more reliably. In fact, a one-subtraction dispersion relation can be formulated which removes the divergence difficulty. (2) Chew and Mandelstam have observed from the crossing relations for pion-pion scattering that a P-wave resonance produces a long-range repulsive force in addition to the shorter range attraction. We represent such an interaction by a "two-pole" P-wave effective-range formula.

To obtain the normalization of the $N\bar{N} \to \pi\pi$ amplitude, we start with the pion-nucleon fixed momentum-transfer dispersion relations in the neighborhood of zero momentum transfer. The projection of the $J=1$, $I=1$ $N\bar{N} \to \pi\pi$ characteristic amplitudes from the dispersion relations yields

$$f_+^1(t) = \frac{1}{p_- q_-}\left\{4f^2m^3 z_0 Q_1(z_0) + \frac{1}{4\pi^2}\int_{(m+1)^2}^{\infty} ds\left[\frac{p_-}{q_-}\,\mathrm{Im}A^{(-)}(s,t) + mz\,\mathrm{Im}B^{(-)}(s,t)\right]Q_1(z)\right\}, \tag{1}$$

$$f_-^1(t) = \frac{\sqrt{2}}{3p_- q_-}\left\{4f^2m^2\left[Q_0(z_0) - Q_2(z_0)\right] + \frac{1}{4\pi^2}\int_{(m+1)^2}^{\infty} ds[\mathrm{Im}B^{(-)}(s,t)][Q_0(z) - Q_2(z)]\right\}, \tag{2}$$

where the notation is that of FF and the Q's are Legendre functions of the second kind.

For sufficiently small t, the functions $A(s,t)$ and $B(s,t)$ can be expressed in terms of pion-nucleon phase-shifts. To suppress the high-energy portion of the integrals in Eqs. (1) and (2), a subtraction can be introduced into the original fixed-t dispersion relations. In the present calculation, we have evaluated the value and the derivative of both f_+ and f_- at $t=0$ in the no-subtraction and the one-subtraction forms. The subtraction was made at the pion-nucleon threshold where the subtraction constants are related to scattering lengths. The results are given in Tables I and II. For convenience these results are given for FF's Γ_1 and Γ_2 which are directly related to the electric and magnetic form factors.

In the evaluation of the integrals, we have expressed ImA (ImB) in terms of combinations of total cross sections and the (3,3) amplitude in such a way that the $J=3/2$ states are taken into account exactly. We believe that such a combination is more accurate than the (3,3) amplitude alone since the second resonance is probably in the $J=3/2$ D state. The scattering lengths used are taken from the analysis of Barnes et al.[3] and Hamilton and Woolcock.[4] It is clear that $\Gamma_1(0)$ is the most accurately determined normalization. The uncertainty in the one-subtraction values of $\Gamma_2(0)$ and $\Gamma_1'(0)$ comes mainly from the inaccuracy of the small P-wave scattering lengths. If the small P-waves are ignored, we find $\Gamma_2(0)=0.0033$ and $\Gamma_1'(0)=0.0348$. Since the D-wave scattering lengths are yet unknown, we can only estimate the order of magnitude of $\Gamma_2'(0)$ from the no-subtraction formula. It may be possible to improve the accuracy of the normalizations by varying the subtraction energy in the pion-nucleon dispersion relation over the region where pion-nucleon phase-shift analyses have been performed.

Table I. Normalizations with no subtraction.

	Born term	Dispersion integral	Total
$\Gamma_1(0)$	-0.159	0.0186	-0.140
$\Gamma_2(0)$	0.0238	-0.0187	0.0051
$\Gamma_1'(0)$	0.0364	0.00224	0.0386
$\Gamma_2'(0)$	-0.00562	0.00107	-0.00455

To obtain the $\Gamma_{1,2}(t)$, we use the dispersion formula given by FF. The left-hand cut of the Γ is calculated in the same manner as FF except that we terminate the rescattering cut at $t=-26\mu^2$ (where the π-N partial wave expansion diverges) and replace all remaining cuts by a pole whose position and residue are adjusted to give the normalized value and derivative at $t=0$. Of course, this phenomenological pole can also compensate for part of the inaccuracy in the rescattering cut. The D function which appears in the FF formula is now represented by

$$D(\nu)=1-\nu[A_1\nu_1K(\nu_1,-\nu)+A_2\nu_2K(\nu_2,-\nu)],$$
$$\nu=\tfrac{1}{4}(t-4\mu^2), \qquad (3)$$

where ν_1 and ν_2 are the positions of the poles in the pion-pion two-pole effective-range formula, and A_1 and A_2 are the corresponding residues. The $K(\nu',-\nu)$ appearing in Eq. (3) is the kernel defined by CM.[2]

Having obtained the Γ's expressed in terms of the pion-pion parameters, one can then calculate the isovector part of the nucleon form factors. A typical set of parameters which fits the observed value and radius of the magnetic moment form factor is $\nu_1=60$, $\nu_2=4$, $A_1=0.3$, $A_2=-0.32$ (in pion units), corresponding to a resonance at $t=12$. Although we have four pion-pion parameters, the value of ν_2 is closely related to the position of the resonance and therefore can be determined by consistency requirements ($\nu_2\simeq 2\nu_1+1$). For three different values of ν_1 ($\nu_1=25$, 40, 60), the variation of the position and width of the resonance was quite small. The two-pion contribution to the charge in these cases was 20% of the total charge. Although the

Table. II. Normalizations with one subtraction at the pion-nucleon threshold.

	Born term	Scattering lengths S	P	D	Dispersion integral	Total
$\Gamma_1(0)$	-0.1055	-0.0339			-0.0012	-0.141
$\Gamma_2(0)$	0.0238	-0.0002	-0.0319		0.0041	-0.0042
$\Gamma_1'(0)$	0.00535	0.00135	0.0382		-0.0019	0.0430
$\Gamma_2'(0)$	-0.00562	-0.0001	-0.0026	?	-0.0004	?

Γ_1 amplitude is still quite sensitive to the uncertainty in the normalizations due to a cancellation, we believe that our solution for it is qualitatively more reliable than the function given by FF.

While we feel that we have made improvements over the FF solution, we find that the value of A_2 required to fit the magnetic moment is too large to be consistent with the CM crossing relations. This indicates that either the pion-pion effective-range formula in its present form is inadequate, or the higher mass intermediate states are non-negligible for both the charge and magnetic form factors.

*This work was performed under the auspices of the U. S. Atomic Energy Commission.

†Part of this work was done while the authors were at the Lawrence Radiation Laboratory, University of California, Berkeley, California.

[1]W. R. Frazer and J. R. Fulco, Phys. Rev. 117, 1603 (1960); 117, 1609 (1960) (hereafter referred to as FF).

[2]G. F. Chew and S. Mandelstam, University of California Radiation Laboratory Report UCRL-9126, March, 1960 (unpublished) (hereafter referred to as CM).

[3]S. W. Barnes, B. Rose, G. Giacomelli, J. Ring, K. Miyake, and K. Kinsey, Phys. Rev. 117, 226 (1960); S. W. Barnes, H. Winick, K. Miyake, and K. Kinsey, Phys. Rev. 117, 238 (1960).

ELECTROMAGNETIC MESON MASS DIFFERENCES

D. J. Hall
Department of Physics, Queen Elizabeth College, London, England
(Received November 28, 1960)

The π-meson and K-meson electromagnetic mass differences have been qualitatively explained by Matthews and Uretsky, and others,[1,2] in terms of a simple classical model. In considering the quantum mechanical analog of their model, Matthews and Uretsky ignored the two-photon vertex term. This is a divergent term, independent of the meson structure, which is known to dominate the pion case in the conventional gauge, and actually to determine the sign of the mass difference. In disperson theory, the pion mass difference has been calculated by Riazuddin[3] who treats this term only very approximately.

It has been suggested by Feldman[4] that the difficulties associated with this term may be avoided by working in the F.E.M. (finite electromagnetic mass) gauge in which it vanishes identically. The purpose of this note is to show that when this is done the remaining term becomes finite in the "pole" approximation to the dispersion relation, and a rather satisfactory quantum theory of both the pion and the K-meson mass splitting is obtained, in terms of physically reasonable electromagnetic form factors.

We write the self-energy arising from the process of lowest order in e^2 shown graphically in Fig. 1(a) as

$$\delta(m^2) = \frac{i}{4\pi^3} \times \frac{1}{4\pi} \int D_{\mu\nu}(q^2) K(p,q) d^4q, \qquad (1)$$

where

$$K(p,q) = i(2E)(2\pi)^3 \times \tfrac{1}{2}\{\int d^4y \, \exp(-iqy)(\langle p|T(j_\mu(y) j_\nu^\dagger(0))|p\rangle - \langle 0|T(j_\mu(y) j_\nu^\dagger(0))|0\rangle$$

$$+ \int d^4y \, \delta(y_0) \exp(-iqy) \overline{\delta}_{y_0} (\langle p|[\dot{A}_\mu(y), j_\nu^\dagger(0)]|p\rangle - \langle 0|[\dot{A}_\mu(y), j_\nu^\dagger(0)]|0\rangle)\} \qquad (2)$$

is the transition matrix element for the scattering of a (real) photon off a boson, and $D_{\mu\nu}(q^2)$ is the virtual photon propagator,

$$D_{\mu\nu}(q^2) = (1/q^2)(g_{\mu\nu} - a q_\mu q_\nu / q^2). \qquad (3)$$

In Eq. (2) we ignore the vacuum expectation terms which contribute equally to the self-masses of charged and uncharged mesons. Taking

$$j_\mu = ie[\phi^\dagger \partial_\mu \phi - \partial_\mu \phi^\dagger \phi] - 2e^2 \phi^\dagger \phi A_\mu, \qquad (4)$$

FIG. 1. Lowest order Feynman diagrams of meson electromagnetic self-energy.

and ignoring possible subtraction terms, we evaluate the remaining terms of $K(p, q)$ in the one-meson approximation. To order e^2,

$$\int d^4y \exp(-iqy)\langle p|T(j_\mu(y)j_\nu^\dagger(0))|p\rangle$$

$$=\frac{1}{(2\pi)^3}\frac{e^2}{2p_0}F_1^2(q^2)\left[\frac{(2p+q)_\mu(2p+q)_\nu}{(p+q)^2-m^2-i\epsilon}+\frac{(2p-q)_\nu(2p-q)_\mu}{(p-q)^2-m^2-i\epsilon}\right], \tag{5}$$

where m is the meson mass, and $F_1(q^2)$ is the form factor arising from the first term in j_μ,

$$\langle p|j_\mu|p'\rangle=-[1/(4p_0p_0')^{1/2}][1/(2\pi)^3]e(p+p')_\mu F_1(q^2).$$

On the other hand, only the e^2 term in j_μ contributes to the equal-time commutator term in Eq. (2),

$$\int d^4y\,\delta(y_0)\exp(-iqy)\dot{\delta}_{y_0}\langle p|[\dot{A}_\mu(y),j_\nu^\dagger(0)]|p\rangle$$

$$=\int d^4y\,2ie^2\exp(-iqy)\langle p|\phi(0)\phi^\dagger(0)|p\rangle\,\delta_{\mu\nu}\delta^4(y)$$

$$=\frac{2ie^2}{(2\pi)^3}\frac{\delta_{\mu\nu}}{2p_0}F_2. \tag{6}$$

Since $F_2=(2\pi)^3(2p_0)\langle p|\phi(0)\phi^\dagger(0)|p\rangle$, the form factor associated with the two-photon vertex, Fig. 1(b), is independent of q^2, the contribution of Eq. (6) to the self-mass will remain infinite for any choice of F_2, unless it is evaluated in the particular gauge in which it vanishes identically.

Combining Eq. (5) and Eq. (6) and substituting into Eq. (1), where the two terms of Eq. (5) give equal contributions,

$$\delta(m^2)=\frac{i}{4\pi^3}\frac{e^2}{4\pi}\int D_{\mu\nu}(q^2)\left[F_1^2(q^2)\frac{(2p-q)_\nu(2p-q)_\mu}{q^2-2pq-i\epsilon}-F_2\delta_{\mu\nu}\right]. \tag{7}$$

Consider the choice of $D_{\mu\nu}(q^2)$ in Eq. (3). In the F.E.M. gauge, $a=4$, and the second term of Eq. (7) vanishes. The remaining term is finite for any reasonable choice of form factor $F_1(q^2)$,

$$\delta(m^2)=\frac{i}{4\pi^3}\frac{e^2}{4\pi}\int d^4q\,F_1^2(q^2)\left[\frac{(2p-q)^2}{q^2(q^2-2pq-i\epsilon)}-\frac{4}{q^2}\right], \tag{8}$$

ignoring a term $8p\cdot q/q^2$ which vanishes in symmetrical integration.[5] Taking[1]

$$F_1^\dagger(q^2)=\lambda^2/(\lambda^2+q^2),\quad F_1^0(q^2)=0 \quad \text{for } \pi \text{ mesons},$$

$$F_1^\dagger(q^2)=\lambda^2/(\lambda^2+q^2),\quad F_1^0(q^2)=[\lambda^2/(\lambda^2+q^2)$$

$$-\mu^2/(\mu^2+q^2)] \quad \text{for } K \text{ mesons},$$

then

$$\delta m_{\pi^+}-\delta m_{\pi^0}=-\frac{\alpha^2}{8\pi m_\pi}\left\{\lambda^2\left(1+\frac{12m_\pi^4}{\lambda^4}-\frac{3}{2}\frac{m_\pi^2}{\lambda^2}\right)-4\lambda^2\right\}\simeq+\frac{3\alpha^2\lambda^2}{8\pi m_\pi}, \tag{9}$$

$$\delta m_{K^+}-\delta m_{K^0}=+\frac{\alpha^2}{8\pi m_K}\left\{\lambda^2\left[\left(\gamma^2-\frac{2\gamma^2}{\gamma^2-1}\ln\gamma^2\right)-\frac{12m_K^4}{\lambda^4}-\frac{3}{2}\frac{m_K^2}{\lambda^2}\right]-4\lambda^2\left(\gamma^2-\frac{2\gamma^2}{\gamma^2-1}\ln\gamma^2\right)\right\}$$

$$\simeq-\frac{3\alpha^2\lambda^2}{8\pi m_K}\left(\gamma^2-\frac{2\gamma^2}{\gamma^2-1}\ln\gamma^2\right). \tag{10}$$

It is well known that the observed positive pion mass difference is obtained from Eq. (9) by taking $\lambda \simeq m_N$, the nucleon mass. In Eq. (10), if we take $\lambda_K \simeq \lambda_\pi = m_N$, then the observed negative mass difference of 3.5 Mev is obtained for $r = \mu/\lambda \simeq 2.5$. (The value of r is rather insensitive to that of λ, varying between 1.8 and 3.0 for all values of λ.) Thus we find a model for the K meson of a positively charged cloud of root mean square radius $\langle a_\lambda \rangle \simeq \langle a_\pi \rangle \simeq 0.5 \times 10^{-13}$ cm, with a negatively charged core of root mean square radius $\langle a_\mu \rangle \simeq 0.2 \times 10^{-13}$ cm.

The author is very much indebted to Dr. P. T. Matthews for suggesting this work and for his continued advice and assistance, and also to Professor A. Salam for the hospitality of the Theoretical Physics Department of Imperial College, London, England.

[1]P. T. Matthews and J. L. Uretsky, Phys. Rev. Letters 3, 297 (1959).

[2]K. Tanaka, Phys. Rev. 117, 1403 (1960).

[3]Riazuddin, Phys. Rev. 114, 1184 (1959).

[4]L. Evans, G. Feldman, and P. T. Matthews (to be published).

[5]This is recognizable as the expression obtained by R. P. Feynman and G. Speisman [Phys. Rev. 94, 500 (1954)] in the conventional gauge using cutoff factors $F_1(q^2)$, and $F_2 = F_1^2(q^2)$. However, while $F_1(q^2)$ may be interpreted as the meson structure term, the q^2 dependence of F_2 introduced to make finite an intrinsically infinite term had no apparent physical basis in their presentation.

ERRATUM

INSTABILITY MECHANISMS IN TRANSVERSE PINCHES. Vernal Josephson, M. H. Dazey, and R. F. Wuerker [Phys. Rev. Letters 5, 416 (1960)].

Due to an unfortunate oversight, the names of the last two co-authors were omitted from the manuscript of this Letter.

ABSTRACTS

In this section are printed the abstracts of Articles that have been forwarded to The American Institute of Physics for publication in THE PHYSICAL REVIEW. In quoting information obtained from this section before the appearance of the corresponding Article, reference should be made to "Physical Review (to be published)" rather than to this Journal.

DIELECTRIC CONSTANT, DENSITY, EXPANSION COEFFICIENT, AND ENTROPY OF LIQUID He^3 UNDER PRESSURE BELOW 1°K. D. M. Lee,* Henry A. Fairbank, and Edward J. Walker, Josiah Willard Gibbs Laboratory, Yale University, New Haven, Connecticut (Received October 25, 1960).

By measuring the resonant frequency of an *LC* circuit containing a capacitor filled with liquid He^3, the dielectric constant of the liquid was measured from 0.15 to 1°K at several pressures from 0.2 to 29.5 atmospheres. From these measurements the density, expansion coefficient at constant pressure, and the change in entropy on compression from saturated vapor pressure to higher pressures were determined. α_p was found to be negative and, hence, $(\partial S/\partial P)_T$ positive for all pressures below a certain temperature which increased monotonically with pressure, confirming behavior found by Brewer and Daunt. A minimum in the melting curve of He^3 was found at $T = 0.32 \pm 0.01$°K and $p = 29.1 \pm 0.1$ atm. The results are compared with those obtained by other methods.

*Now at Cornell University, Ithaca, New York.

QUANTUM-CORRECTED STATISTICAL METHOD FOR MANY-PARTICLE SYSTEMS: DENSITY MATRIX. L. C. R. Alfred, Brookhaven National Laboratory, Upton, New York (Received October 19, 1960).

Quantum corrections are obtained for the single-particle density matrix in a semiclassical ensemble where the distribution is unrestricted. A form for the density matrix containing explicitly a function of the wave-mechanical Hamiltonian operator is devised; a formalism is then developed to decompose this operator function into effectively classical and nonclassical parts. The classical part corresponds to the semiclassical density matrix and the quantum corrections are obtained from the nonclassical terms.

The quantum-corrected density matrix for a spherically symmetrical and one-dimensional system have been evaluated. The densities for a linear harmonic oscillator and a Coulomb potential for a Fermi-Dirac distribution have also been examined in some detail.

MODES OF ATOMIC MOTIONS IN LIQUID HELIUM BY INELASTIC SCATTERING OF NEUTRONS. D. G. Henshaw and A. D. B. Woods, Division of Physics, Atomic Energy of Canada Limited, Chalk River, Ontario, Canada (Received October 27, 1960).

The wavelength distribution of 4.03$_9$A neutrons scattered inelastically by specimens of liquid helium has been measured at 30 angles of scattering in the range 10° to 140°. At each angle of scattering there is a discrete peak with little broadening and only little, if any, excess scattering past the maximum even at the largest angle of scattering. The corresponding change in energy and momentum of the scattering neutrons has been calculated from the change in wavelength and the angle of scattering. The dispersion curve in the liquid is similar in form to that predicted theoretically but there are differences in detail. For momenta in the range $0.26\ A^{-1} \leq Q \leq 0.6\ A^{-1}$, the measurements are consistent with the phonon branch theoretically predicted from the known measured velocity of sound. The maximum and the minimum of the curves occur at $1.10\ A^{-1}$ and 13.7°K and at $1.91\ A^{-1}$ and 8.65°K, respectively. Beyond the minimum the curve starts to rise with a slope equal to or less than the phonon branch and then falls below this, suggesting the possible existence of a theoretically unpredicted second maximum. The relative partial differential cross section for the production of a single-phonon excitation is low at low momenta, has a maximum in the region of $2.0\ A^{-1}$, and then decreases rapidly to low values in the region of $2.68\ A^{-1}$. The position of the maximum may be compared with $2.05\ A^{-1}$ and $1.91\ A^{-1}$, the maximum in the total differential cross section curve and the minimum of the dispersion curve, respectively. The widths and mean energy change of neutrons scattered through 80° have been measured at 13 temperatures in the range 1.78°K to 4.21°K. Scattering at this angle corresponds to the production of excitations at the minimum

of the dispersion curve. The mean energy change decreases rapidly from a value of 8.6_5°K at 1.1°K to 5.6°K at the λ temperature, where there is a marked, theoretically unpredicted, change in slope, and only a much slower decrease above the λ temperature to 4.9°K at 4.2°K. The widths of the spectra increase rapidly from a value of <1°K at 1.1°K to 11°K at the λ temperature, where there is also a marked, theoretically unpredicted, change in slope, and only a much slower increase to about 5°K at 4.2°K. The measured widths are compared with theoretically calculated widths.

THEORY OF THE de HAAS–van ALPHEN EFFECT FOR A SYSTEM OF INTERACTING FERMIONS. J. M. Luttinger, Department of Physics, Columbia University, New York, New York (Received October 17, 1960).

The de Haas–van Alphen effect for a system of interacting fermions is investigated. It is shown that, granting certain analytic properties (which were used before in establishing the existence of a Fermi surface, and which have only been established in the sense of perturbation theory), it is possible to obtain a simple expression for the oscillatory part of the thermodynamic potential. In particular, one finds that the de Haas–van Alphen oscillations have the same amplitude and period as in the usual quasiparticle picture, but that the phase is given by a more complicated procedure.

LOW-TEMPERATURE PHOTOCONDUCTIVITY OF ADDITIVELY COLORED KCl. Robert L. Wild and Frederick C. Brown, Department of Physics, University of Illinois, Urbana, Illinois (Received October 17, 1960).

The transient photoconductivity of additively colored crystals of KCl has been investigated at temperatures down to 10°K. The spectral response reflects the structure in optical absorption in the ultraviolet reported by Lüty. Quantum yields are found to be less than 1.0 at 10°K but are much higher in the region of the L_1 (3.6 ev) and L_2 (4.2 ev) bands than in the K band on the high-energy side of the F band. The beginning of electron collection or saturation effects was found in the case of thin, lightly colored crystals which indicates that electron ranges were in the vicinity of 10^{-6} cm²/volt at 10°K. Shallow traps effective below 26°K were found in the crystals studied so far. These traps have a large product of concentration times cross section and compete favorably with the F center at 10°K. They can be partly filled following illumination at low temperature, with the result that enhanced photoresponse is produced in the red and near infrared.

PHOTOELECTRIC HALL EFFECT IN KCl AT LOW TEMPERATURES. Frederick C. Brown and Nicolas Inchauspe,* University of Illinois, Urbana, Illinois (Received October 17, 1960).

The Hall effect for carriers released by light has been studied over a temperature range 4° to 114°K in additively colored crystals of KCl containing various concentrations of F centers. A negative Hall signal was observed corresponding to electrons released from F centers by light absorbed in the high-energy side of the F band. The Hall mobility rises steeply below 80°K due to freezing out of the optical modes of lattice vibration. A residual mobility near 4000 cm²/volt sec is found below 30°K in the crystals prepared so far.

*Present address: Societé Nationale Petroles d'Aquitaine, 16 Cours Albert, Paris, France.

DIFFUSION IN COMPOUND SEMICONDUCTORS. B. Goldstein, Radio Corporation of America Laboratories, Princeton, New Jersey (Received September 27, 1960).

Self-diffusion in single-crystal InP and GaAs has been measured, together with the diffusion of the acceptors Cd and Zn and the donors S and Se in GaAs. Radioactive isotopes of these elements were used as tracers. The diffusions of In and P in InP are characterized by activation energies of 3.85 ev and 5.65 ev, respectively; those for Ga and As in GaAs are characterized by activation energies of 5.60 ev and 10.2 ev, respectively. The marked differences in both activation energies and diffusion rates of the constituent atoms in these materials indicate that the basic mechanism of the self-diffusion is one of migration within a specific sublattice.

The impurity diffusion measurements in GaAs suggest that the concept of sublattice diffusion be extended to include impurity diffusion when the impurities enter the lattice substitutionally.

The activation energy of the diffusion of both Cd and Zn in GaAs is about 2.5 ev, while that of the diffusion of both S and Se in GaAs is about 4.1 ev. Experimental details of interest include the observation of GaS compound formation when GaAs is heated in S vapor, and the formation of glassy layers on the surface of GaAs due to Se.

APPROXIMATE CALCULATION OF THE ANISOTROPY OF THE RELAXATION TIME OF THE CONDUCTION ELECTRONS IN THE NOBLE METALS. J. M. Ziman,* General Electric Research Laboratory, Schenectady, New York (Received October 31, 1960).

The ratio of the relaxation times on the "belly" and on the "necks" of the Fermi surface is estimated numerically by very crude methods. It is shown that the relative amount of s-wave to p-wave scattering by impurities is important and that Umklapp processes play a major role in phonon scattering. The ratio depends on impurity type and on temperature in just the right way to explain qualitatively the variation of the Hall coefficient in the metals and their alloys.

*Permanent address: Cavendish Laboratory, University of Cambridge, Cambridge, England.

EFFECT OF A CONSTANT ELECTRIC FIELD ON GERMANIUM FAST SURFACE STATES. Y. Margoninski,* Barus Physics Laboratory, Brown University, Providence, Rhode Island (Received August 25, 1960).

The experimental evidence regarding the effect of electric fields on the fast states of germanium is, at present, contradictory: Litovchenko and Lyashenko explained their experimental results by assuming that the fields affect only the density of states but not their energy; this would support the current view on charge transfer through the semiconductor oxide layer. Rzhanov et al., on the other hand, reported field-induced changes in energy as well as density. To resolve this question, careful measurements of surface recombination velocity and surface conductivity were performed before and after application of dc fields of about 2×10^6 volts/cm. Though the effect of the field on the surface state density was much smaller than that found by Litovchenko and Lyashenko, the experimental results indicated clearly that the energy and ratio of capture cross sections were indeed unaffected by the field. It was also found that in wet ambients the ac field shifted the unperturbed surface potential by more than $+5kT$.

*On leave from the Department of Physics, Hebrew University, Jerusalem, Israel. Present address: Research Laboratory, Raytheon Company, Waltham, Massachusetts.

ELECTRON SPIN-LATTICE RELAXATION OF CHROMIUM IN MgO. J. G. Castle, Jr. and D. W. Feldman, Westinghouse Research Laboratories, Pittsburgh, Pennsylvania (Received October 31, 1960).

The effective spin-lattice relaxation time, T_1, has been observed for the ground-state multiplet of Cr(+3) in the cubic field of MgO. T_1 is observed to vary from 800 milliseconds at 1.3° to 3.4 milliseconds at 50°K. The direct process dominates below 4.2°.

DISTRIBUTION OF FIELDS FROM RANDOMLY PLACED DIPOLES: FREE PRECESSION SIGNAL DECAY AS RESULT OF MAGNETIC GRAINS. Robert J. S. Brown, California Research Corporation, La Habra, California (Received October 21, 1960).

Free precession signals were observed from fluids in samples containing randomly distributed ferromagnetic grains. The local free precession phase shift was calculated by computing volumes of space for various ranges of perturbing field strength near individual grains. The frequency of occurrence of a given phase shift caused by individual grains is inversely proportional to the square of the phase shift, this distribution being a limiting case of the Cauchy form. The resultant distribution of phase shifts from effects of many grains is then still of the Cauchy form. This leads to an exponential signal decay, with the rate independent of diffusion. If M is the algebraic sum of the individual dipole moments of the individual magnetic grains per unit volume, and γ the magnetogyric ratio, then $1/T_2 = (8\pi^2/9\sqrt{3})M\gamma$ if all grains are magnetized parallel to the precession field; $1/T_2 = (4\pi/3)M\gamma$ if perpendicular. Within 10%, $1/T_2 = 4.6M\gamma$ for any random or systematic orientation of the grains. Measurements on water containing magnetite powder stabilized by carboxymethylcellulose and

on glycerine containing magnetite powder, as well as on sands containing magnetite powder and saturated with water or glycerine, verified the exponential decay, independence of decay rate on diffusion or viscosity, and the above numerical value of decay rate (with small geometrical correction applied to results for the sand system).

FERROMAGNETIC RELAXATION CAUSED BY INTERACTION WITH THERMALLY EXCITED MAGNONS. Ernst Schlömann, Research Division, Raytheon Company, Waltham, Massachusetts (Received July 25, 1960).

The contribution of three-magnon processes to the relaxation rate of spin waves is investigated. Relaxation occurs through the confluence of two magnons (with the generation of a third magnon), and through the splitting of a magnon into two magnons. The relaxation rate due to the confluence process is approximately proportional to the wave number, whereas that due to the splitting process is approximately independent of the wave number. The latter contribution vanishes at frequencies higher than $\frac{2}{3}\gamma 4\pi M$ (γ = gyromagnetic ratio, M = saturation magnetization), and increases with decreasing frequency. The implications of the theory with respect to the observation of spin-wave instability in an rf magnetic field parallel to the dc field are discussed.

MAGNETIC INTERACTION OF CERIUM AND COBALT IONS IN DOUBLE NITRATE CRYSTALS. J. W. Culvahouse, W. Unruh, and R. C. Sapp, Department of Physics and Astronomy, University of Kansas, Lawrence, Kansas (Received August 22, 1960).

The space group of the double nitrate crystals $M_2'M_3''(NO_3)_{12}\cdot 24H_2O$, where M' is a trivalent cation and M'' is a divalent cation, has been determined from x-ray data to be $R\bar{3}m$. The rhombohedral unit cell has sides of 13.9 A, interaxial angles of 49° and contains one molecule. The cerium ions have the location $\pm(\frac{1}{4},\frac{1}{4},\frac{1}{4})$. The line shapes of the derivative with respect to the magnetic field of the paramagnetic resonance absorption of small concentrations of cobaltous ions substituted in $Ce_2Zn_3(NO_3)_{12}\cdot 24H_2O$ are described and used to determine the spatial relations of the cerium ions and cobalt ions, as well as to justify the assumption of a dipolar interaction between them described by the spin Hamiltonian parameters of the cerium and cobalt ions. It is concluded that the more isotropic of the two paramagnetic spectra of cobalt ions observed in this salt is due to ions in either the special sites $\pm(0.399, 0.399, 0.399)$ or, rather less likely, in the special sites $\pm(0.101, 0.101, 0.101)$, and that the highly anisotropic spectrum of cobalt ions is due to ions in the body-centered site.

d BANDS IN CUBIC LATTICES. III. Joseph Callaway, Westinghouse Research Laboratories, Pittsburgh, Pennsylvania and Division of Physical Sciences, University of California, Riverside, California (Received October 17, 1960).

A simple model of an ionic crystal is considered, consisting of a lattice of point charges (Z_1e) and (Z_2e) arranged in the rock-salt structure, and screened by a uniform distribution of negative charge. This lattice defines a periodic potential in which electron energy levels are calculated. The energies of five states pertaining to the *d* band are calculated, by expansion in symmetrized combinations of plane waves, as functions of the average binding and relative ionicity.

INFRARED LATTICE BANDS OF QUARTZ. W. G. Spitzer and D. A. Kleinman, Bell Telephone Laboratories, Murray Hill, New Jersey (Received October 24, 1960).

The infrared lattice bands of α quartz have been investigated at 297°K from 5 to 37 μ in reflection and transmission with polarized light. Previously published measurements of the optical constants do not agree in this spectral range. It is shown that dispersion theory can fit the data within experimental error throughout the range, and accurate values of the dispersion parameters and the optical constants are obtained. This is the first accurate dispersion analysis of a complex spectrum. A study was made of the accuracy of the Kramers-Kronig method of analysis on this spectrum. The strength, width, and frequency of 14 optically active lattice vibrations are given, 4 of which have not previously been established. From a consideration of published Raman data 10 of the resonances are assigned according to symmetry type as fundamental vibrations.

SUSCEPTIBILITIES AND NEGATIVE KNIGHT SHIFTS OF INTERMETALLIC COMPOUNDS. A. M. Clogston and V. Jaccarino, Bell Telephone Laboratories, Murray Hill, New Jersey (Received October 19, 1960).

Knight-shift measurements have recently been made on a series of compounds of the β wolfram structure V_3X, namely V_3As, V_3Au, V_3Ga, V_3Ge, V_3Pt, V_3Sb, V_3Si, and V_3Sn. More recently susceptibilities have been measured on some of these compounds. It is observed that (a) materials with a high superconducting transition temperature show temperature-dependent Knight shifts and susceptibilities, (b) the vanadium shifts K_V are positive and decrease with decreasing temperature, and (c) the X-site shifts K_X are negative and increase in magnitude with decreasing temperature. A simple model will be offered which uses the Heine exchange polarization mechanism to relate the sign and temperature dependence of K_V and K_X to the temperature-dependent susceptibility.

COLLISION THEORIES OF CATHODE SPUTTERING OF METALS AT LOW ION ENERGIES. Erich B. Henschke, Electronic Technology Laboratory, Wright Air Development Division, Air Research and Development Command, United States Air Force, Dayton, Ohio (Received December 15, 1959; revised manuscript received April 14, 1960).

The periodicity of the threshold energies, as seen in a plot vs atomic number, is more pronounced for threshold energies determined from the part of the yield curve at the lowest ion energies, which obeys a quadratic law, than for "cut-in" energies determined with a linear law from the adjacent somewhat higher ion energy range. The relationship of the "empirical sputtering relation" of Wehner with the threshold formula, formerly derived by the author, is clarified. It is shown that in the case that the rebounding particle is believed to be a displaced target atom, the assumption of a very large "effective" mass of the struck atom must also be made to explain the rebound at angles as observed in ejection patterns of single-crystal planes. Arguments are presented that the author's model is consistent with the observed higher yields of metals with completely filled d shells, such as Cu, Ag, and Au.

The energy losses connected with the impulses used up in Debye waves, as assumed in the author's theory, are shown to be in good agreement with Silsbee's calculations of the energy losses in similar collisions.

APPEARANCE AND EFFECT OF THE DEBYE-WALLER FACTOR IN THE TRANSPORT COEFFICIENTS OF SIMPLE NORMAL METALS. M. Bailyn, Northwestern University, Evanston, Illinois (Received July 13, 1960; revised manuscript received November 7, 1960).

Analogous to the theory of the diffraction of x rays and neutrons by the lattice vibrations of crystals, the scattering of electrons in a metal by thermal vibrations gives rise to a temperature-dependent Debye-Waller factor in the matrix element. The factor is derived and its possible effects on electrical resistivity discussed for the case where Bloch functions are used for the electron wave function. A detailed numerical calculation for an umklapp process involving a particular phonon was performed, with the result that the new matrix element is about 0.7 times the 1937 Bardeen result, and consequently the contribution to the resistivity is about 0.5 times the Bardeen value. It is even a possibility that, for some phonons, the matrix element may increase.

MÖSSBAUER EFFECT WITH Ni^{61}. Felix E. Obenshain and Horst H. F. Wegener,* Oak Ridge National Laboratory, Oak Ridge, Tennessee (Received October 21, 1960).

The Mössbauer effect is observed in Ni^{61}. The Ni^{61*} was obtained by $Ni^{64}(p,\alpha)Co^{61}\xrightarrow{\beta^-(99\ \mathrm{min})}Ni^{61*}$, giving a nickel Mössbauer nucleus in a Ni^{64} host lattice. The magnitude of the effect at $T=80°K$ is about 4% for a 400-mg/cm^2 absorber foil (natural nickel). From the thickness dependence we obtain $f_{source}=f_{abs}=(9\pm1)\%$ for the Debye-Waller factor at $T=80°K$. The temperature dependence yields a Debye temperature varying between 413° and 437°K. The velocity dependence has a half-width of 1.65 mm/sec. The spectrum deviates from the Lorentz shape expected for a single line. A recent electronic determination of the lifetime of this 71-kev state indicates a natural half-width of 0.37 mm/sec. The increased half-width and shape of the spectrum observed in our experiment may be understood in terms of a magnetic hyperfine splitting. The moment of the

ground state is known. The internal field H and the magnetic moment μ_e of the first excited state are unknown. An analysis of the data gives a connection between the two quantities, $\mu_e(H)$.

*On leave from University of Erlangen, Erlangen, Germany.

FINE STRUCTURE OF SECONDARY EMISSION vs ANGLE OF INCIDENCE OF THE PRIMARY BEAM ON TITANIUM SINGLE CRYSTALS. R. W. Soshea* and A. J. Dekker,† Department of Electrical Engineering, University of Minnesota, Minneapolis, Minnesota (Received May 16, 1960; revised manuscript received November 21, 1960).

The secondary emission ratio of single crystals of titanium has been measured as a function of the angle of incidence of the primary electron beam. The curves show a general increase of the secondary emission ratio with increasing angle between the electron beam and the normal to the crystal face. Superimposed upon this general increase are a number of small relative maxima. The larger and broader of these maxima occur whenever the primary beam is incident along one of the major zone axes of the crystal. The magnitudes of these bands vary with the energy of the incident electrons, but their angular position is independent of energy. The smaller, extremely narrow bands do not correspond to major zone axes of the crystal. Both the magnitude and angular position of these latter peaks vary with the primary energy. The origin of these bands is explained in terms of diffraction of the incident electrons by the crystal lattice.

*Now at Rheem Semiconductor Corporation, Mountain View, California.

†Now at Institute for Crystal Physics Melkweg, Groningen, the Netherlands.

INFLUENCE OF ERGODIC BEHAVIOR ON THE SCATTERING OF SLOW NEUTRONS BY A HARMONIC OSCILLATOR. Theodore J. Krieger,* Brookhaven National Laboratory, Upton, New York (Received October 18, 1960).

Random quantum jumps of a harmonic oscillator in contact with a temperature bath are shown to give rise to a general broadening of the slow-neutron scattering peaks. An exception occurs in the case of the elastic scattering peak, a major component of which remains unbroadened. In general, the broadening increases with the number of quanta transferred. The analysis is based on the "damped" oscillator model of Senitzky.

*Permanent address: Republic Aviation Corporation, Farmingdale, New York.

IONIZATION OF LITHIUM BY FAST PROTONS AND ELECTRONS. M. R. C. McDowell,* Physics Department and Engineering Experiment Station, Georgia Institute of Technology, Atlanta, Georgia, and G. Peach,† Mathematics Department, Royal Holloway College, University of London, London, England (Received August 8, 1960; revised manuscript received November 9, 1960).

Born's approximation is used to calculate the cross sections for ionization of lithium by fast protons (< 1 Mev) and electrons (< 1 kev). The electron impact results are in good agreement with those obtained by Seaton's method from experimental photoionization data. The maximum cross section for proton impact is $1.1\pi a_0^2$ at 20 kev.

*On leave of absence from Royal Holloway College, University of London, London, England, 1959-60.

†Now at Physics Department, University College, London, England.

ELECTRON TEMPERATURE DEPENDENCE OF THE RECOMBINATION COEFFICIENT IN PURE HELIUM. C. L. Chen,* C. C. Leiby, and L. Goldstein, Department of Electrical Engineering, University of Illinois, Urbana, Illinois (Received May 20, 1960; revised manuscript received November 21, 1960).

The phenomenon of "afterglow quenching" is employed to determine the electron temperature dependence of the electron-ion recombination coefficient in plasmas produced in purified helium (estimated impurity $1:10^9$). The total visible light intensity was studied as a function of electron temperature. By means of 1.5% bandwidth filters, the light intensity of two helium spectral lines (5876 A and 3888 A) was also investigated. It is found that the recombination coefficient for highly purified helium varies as the minus three-halves power of the electron temperature from 300° to ~1500°K at electron densities of $\sim 10^{11}$/cc, and gas pressures from

12.6 to 30.3 mm Hg. At 300°K (temperature determined from collision frequency measurements), the recombination coefficient in purified helium is found to be $(8.9\pm0.5)\times10^{-9}$ cm^3/ion-sec. It is found that both the recombination coefficient and its electron temperature dependence were strongly influenced by the addition of controlled amounts (2×10^{-4} to 1300×10^{-4}%) of neon impurities.

*Present address: Coordinated Science Laboratory, University of Illinois, Urbana, Illinois.

LIFETIMES OF EXCITED STATES OF NUCLEI WITH ODD MASS. R. E. Holland and F. J. Lynch, Argonne National Laboratory, Lemont, Illinois (Received October 24, 1960).

The lifetimes of Coulomb-excited states in Ti^{47}, Mn^{55}, Fe^{57}, Zn^{67}, Ge^{73}, Se^{77}, and Mo^{95} have been measured by a pulsed-beam technique. The observed mean lifetimes were between 0.1 and 12.7 mμsec. By combining these data with the measured Coulomb-excitation cross sections, we obtained the partial mean life for magnetic-dipole radiation and the ratio ($E2/M1$) for these transitions. The partial $M1$ lifetimes are 20 to 200 times as long as the single-particle estimates.

NUCLEAR STRUCTURE STUDIES IN THE TIN ISOTOPES WITH (d,p) AND (d,t) REACTIONS. Bernard L. Cohen and Robert E. Price, Radiation Laboratory, University of Pittsburgh, Pittsburgh, Pennsylvania (Received July 22, 1960).

The neutron single-particle states in the odd isotopes of tin are identified by (d,p) angular distribution studies. The cross sections for exciting these states by (d,p) and (d,t) reactions are measured, and the results are analyzed to give values of V_j^2 (in Kisslinger-Sorenson notation), the fraction by which each of the single-particle states is full, for each subshell in each isotope. These are used to calculate ϵ_j, the unperturbed single-particle energies; the results are reasonably consistent. If the observed energies of single-particle states are used to predict the V_j, the agreement is generally good, but some discrepancies are noted and an explanation is offered.

Other weakly excited states are found in the region of the single-particle states. At higher excitation energies, several rather sharp levels are strongly excited in (d,p) reactions. Their energy, cross section, and regularities among the isotopes suggest that these are single-particle levels from the next major shell ($82<N\leq126$); however, their angular distributions cannot be used for identification as they are the same for all levels in this region and show little structure. This last fact is not easily explained.

Some of the two quasi-particle excitation states in the even isotopes of Sn are identified and the apparent pairing energy is thereby measured; it is surprisingly found to vary rapidly with mass number. Spectra from (d,p) and (d,t) reactions in isotonic pairs Cd^{114}-Sn^{116} and Cd^{116}-Sn^{118} are compared to show that the single-particle neutron states are much more radically affected by the addition of two protons than by the addition of two neutrons, contrary to the usual assumption in shell-model theory.

Q values for (d,p) and (d,t) reactions on the major isotopes of tin are measured.

CHARGE DISTRIBUTION IN THE FISSION OF URANIUM ISOTOPES INDUCED BY 20-40 Mev HELIUM IONS. L. J. Colby, Jr. and J. W. Cobble, Department of Chemistry, Purdue University, Lafayette, Indiana (Received March 28, 1960; revised manuscript received November 21, 1960).

The primary yields of Br^{82}, I^{130}, La^{140}, Pr^{142}, and I^{135} have been accurately determined for the medium energy (20-40 Mev) helium-ion-induced fission of U^{233}, U^{235}, and U^{238}. These accurate primary yield data have been correlated with the constant-charge-ratio rule for nuclides away from the neutron shells and give a smooth, but different, distribution curve for nuclides of 83 neutrons.

HELIUM-ION-INDUCED FISSION CROSS SECTIONS OF U^{233} AND U^{238} AND THE NUCLEAR RADII OF HEAVY ELEMENTS. L. J. Colby, Jr., Mary LaSalle Shoaf, and J. W. Cobble, Department of Chemistry, Purdue University, Lafayette, Indiana (Received March 28, 1960; revised manuscript received November 21, 1960).

New radiochemical data of the total fission cross sections have been obtained for U^{233} and U^{238}, which can be used to derive nuclear radii

for these isotopes. This and certain accurate previous results on U^{235} and natural bismuth can be interpreted in terms of an r_0 value of 1.41 $\times 10^{-13}$ cm, when $R_\alpha = 2.19 \times 10^{-13}$ cm, using the Weisskopf square-well nuclear model. Further, the nuclear radii obtained by this analysis are also in good agreement with the radii obtained by others from alpha-particle scattering data with a similar model. A diffuse-potential nuclear model proposed by Igo shows agreement with experiment in the lower energy range. The agreement, however, is not observed with data for higher energies. Certain features of the U^{233} fission curves are also discussed.

RANGE OF 2- TO 60-kev RECOIL ATOMS IN Cu, Ag, AND Au. V. A. J. van Lint, R. A. Schmitt, and C. S. Suffredini, John Jay Hopkins Laboratory for Pure and Applied Science, General Atomic Division of General Dynamics Corporation, San Diego, California (Received October 13, 1960).

The ranges of atoms recoiling from photoneutron reactions in Cu, Ag, and Au have been measured utilizing foil-sandwich irradiations followed by standard radiochemical detection techniques. Different energy spectra of recoil atoms were achieved by varying the bremsstrahlung energy and the angle of emission relative to the incident photons. The results have been compared with calculations of Holmes and Leibfried. The best fit to the data is achieved by assigning values of the multiplicative parameter of the screening radius, α, equal to 1.7 for Cu, 2.0 for Ag, and 3.0 for Au.

GAMMA-RAY CORRELATION FUNCTION IN THE ADIABATIC APPROXIMATION. J. S. Blair and L. Wilets, University of Washington, Seattle, Washington (Received October 13, 1960).

The gamma-ray correlation function following inelastic excitation of an even-A nucleus by a spinless projectile has been analyzed employing only the adiabatic approximation and theorems relevant to elastic scattering. The direction making equal angles with the incident and scattered directions in the scattering plane, the adiabatic recoil direction, is a convenient axis for quantization. In particular, the intermediate (excited) nucleus is populated with only even M states, from which it follows that the gamma distribution is unchanged by a rotation of π about this axis. For a 0^+-2^+-0^+ excitation de-excitation, the gamma distribution in the scattering plane reduces to the form $\sin^2[2(\theta_\gamma - \theta_0)]$, where θ_0 is the adiabatic recoil axis. Comparison is made to the similar predictions of plane-wave Born approximation theories (in which the recoil direction for finite energy transfer is the symmetry axis) and to distorted-wave Born approximation calculations (for which in general there is no simple expression for the symmetry axis). Analysis of experiments verifies the general features of the model, but further data obtained from forward scattering would be desirable to distinguish between the predictions of the adiabatic and Born approximations. Brief comments are made regarding gamma-ray polarization.

QUANTUM MECHANICAL THREE-BODY PROBLEM. II. Leonard Eyges, Lincoln Laboratory, Massachusetts Institute of Technology, Lexington, Massachusetts (Received July 6, 1960).

We present a method for treating the following quantum mechanical three-body problem: to find the ground-state eigenvalue and eigenfunction for a system of three identical particles between any pair of which there is an attractive central force. An essential point of the method is to assume that the wave function Ψ has a special analytic form, $\Psi = \psi(\vec{r}_{12}, \vec{\rho}_3) + \psi(\vec{r}_{13}, \vec{\rho}_2) + \psi(\vec{r}_{23}, \vec{\rho}_1)$, where $\vec{r}_{12} = \vec{r}_1 - \vec{r}_2$, $\vec{\rho}_3 = \vec{r}_3 - \frac{1}{2}(\vec{r}_1 + \vec{r}_2)$, and $\vec{r}_{13}$, $\vec{\rho}_2$ and $\vec{r}_{23}$, $\vec{\rho}_1$ are defined analogously. The Schrödinger equation for the system can then be written as an integral equation for $\phi(\vec{k}, \vec{\kappa})$, the Fourier transform of ψ. We expand this in Legendre polynomials,

$$\phi(\vec{k}, \vec{\kappa}) = \sum_{l=0}^{\infty} \phi_l(k, \kappa) P_l(\cos\gamma),$$

and this yields a set of coupled integral equations for the $\phi_l(k, \kappa)$. These can be truncated and to a good approximation one can neglect all ϕ_l except ϕ_0, thereby reducing the problem to a single integral equation for a function of two variables.

We propose an iterative scheme for solving this equation for the ground-state eigenfunction, and suggest a simple but accurate nonvariational method for deriving the energy eigenvalue therefrom. We test this proposed solution by working

it out in detail for the case of exponential interparticle potentials. The results for the eigenvalue compare favorably with variational calculations by other authors. Finally, we discuss the accuracy of the approximations and the possible sources of error in the wave function.

MAGNETIC MOMENT AND HYPERFINE STRUCTURE COUPLING OF THE FIRST 2+ STATE IN Gd^{154}. Rae Stiening and Martin Deutsch, Department of Physics and Laboratory for Nuclear Science, Massachusetts Institute of Technology, Cambridge, Massachusetts (Received October 21, 1960).

The g value of the 0.123-Mev 2+ state of Gd^{154} is found to be $g = 0.36 \pm 0.06$. The hyperfine structure constant of the same nuclear state in the $^8S_{7/2}$ ground state of Gd^{3+} in aqueous solution is determined as $a = 26.4 \pm 5$ Mc/sec. The perturbation of the angular correlation of gamma-ray cascades proceeding through this state was studied. It is found that the perturbation in aqueous solution can be decoupled by magnetic fields either parallel to one of the gamma rays or perpendicular to the plane of observation. The perturbation in molten $GdCl_3$ is found to be much weaker than in solution and to be unaffected by magnetic fields. Auxiliary measurements involving the first 2+ states in Sm^{152} and Gd^{156} are described.

DECAY OF Hf^{180m}. W. F. Edwards* and F. Boehm, California Institute of Technology, Pasadena, California (Received October 26, 1960).

The energies and relative intensities of the gamma radiation and the relative intensities of the conversion electrons following the decay of 5.5-hr Hf^{180m} have been measured using the curved-crystal gamma-ray spectrometer (recently calibrated for accurate intensity measurements), the ring-focused beta-ray spectrometer, and the semicircular spectrometer at the California Institute of Technology. The measured transition energies are: 57.54 ± 0.01, 93.33 ± 0.02, 215.25 ± 0.13, 332.5 ± 0.3, and 443.8 ± 0.6 kev. The energy levels deduced from these values are not entirely consistent with the two-parameter rotational formula. Conversion coefficients derived from the measurements were absolutely normalized using a method involving information available from the decay scheme. All of the 57.54-kev transition conversion coefficients are anomalously high if compared with the theoretical $E1$ coefficients. No admixture of $M2+E3$ can account for the anomaly. The K conversion coefficients of the $E2$ transitions are all about 10% low with exception of the 93.33-kev transition. The L coefficients have a varying deviation, the maximum being 12%. The K conversion coefficient of the 501.3-kev transition has the value 0.037 ± 0.012 which is consistent with the theoretical $E3$ value of 0.040.

*Present Address: Utah State University, Logan, Utah.

ELASTIC SCATTERING OF POLARIZED 10-Mev PROTONS BY COMPLEX NUCLEI. L. Rosen, J. E. Brolley, Jr., and L. Stewart, Los Alamos Scientific Laboratory, University of California, Los Alamos, New Mexico (Received September 9, 1960).

A systematic investigation has been carried out on the angular dependence of the polarization in the elastic scattering of 10-Mev protons by complex nuclei. Strong polarization effects, which vary smoothly with scattering angle and atomic number of target nucleus, appear to be a general feature of the scattering process. All the data are fitted reasonably well by a 5-parameter "optical model potential" (containing a spin-orbit term) in which the only variable is the $A^{1/3}$ dependence of the radius. The strength of the spin-orbit term required to account for the polarization is approximately the same as has been postulated in the shell model.

RADIOCHEMICAL STUDY OF THE RANGES IN METALLIC URANIUM OF THE FRAGMENTS FROM THERMAL NEUTRON FISSION. James B. Niday, Lawrence Radiation Laboratory, University of California, Livermore, California (Received September 23, 1960).

The mean ranges in uranium of 28 fission products have been determined by radiochemical measurement of the fraction escaping from the surface. Several factors affecting the precision and accuracy of the method are discussed. A semiempirical equation was developed which gave an excellent correlation between the ranges of fragments from a specific mass chain and

their average initial velocity. The average total kinetic energy of the fragment pairs is about 30 Mev less for the products of symmetrical fission than is expected from comparison with the asymmetrical products. The low momenta of the symmetrical fragments are not readily explained by particle emission unless the concept of isotropic neutron evaporation is abandoned. The results may be interpreted by assuming that the symmetrical and asymmetrical products result from two modes of fission which involve different critical shapes of the fissioning nucleus, and that the choice between modes is dependent on the closing of the 50-proton shell in the heavy fragment. The 10% decrease in range observed for two shielded nuclides is also examined in some detail.

$(n, 2n)$ EXCITATION FUNCTIONS OF SEVERAL NUCLEI FROM 12.0 TO 19.8 Mev. R. J. Prestwood and B. P. Bayhurst, Los Alamos Scientific Laboratory, University of California, Los Alamos, New Mexico (Received October 3, 1960).

$(n, 2n)$ excitation functions have been obtained for Sc^{45}, Ti^{46}, Ni^{58}, Cu^{65}, Ge^{70}, As^{75}, Rb^{85}, Rb^{87}, Sr^{84}, Y^{89}, Zr^{90}, Nb^{93}, Ag^{107}, In^{115}, Sn^{112}, Sb^{121}, Sb^{123}, Ta^{181}, Au^{197}, Tl^{203}, and Th^{232} at incident neutron energies of 12.00 to 19.76 Mev. The target elements were exposed to neutrons from the $T(d,n)He^4$ reaction in Zr-T and T_2 gas targets, and the products were measured by radiochemical methods.

$Si^{28}(p, p'\gamma)$ ANGULAR CORRELATIONS. H. F. Bowsher,* G. F. Dell, and H. J. Hausman, Department of Physics, The Ohio State University, Columbus, Ohio (Received October 24, 1960).

Angular correlations have been measured between protons scattered inelastically from a Si^{28} target and the decay gamma rays from the 1.78-Mev first excited state of the target nuclei. The incident proton bombarding energy was varied between 5.8 Mev and 7.0 Mev. The angular correlation experiments were performed for proton detector angles of 37°, 60°, 90°, and 120°. The measured angular correlation functions are all of the form $A + B \sin^2[2(\theta - \theta_0)]$, where θ_0 is the axis of symmetry. When the incident proton beam energy was 7.0 Mev, the symmetry direction was found to be 90° (center-of-mass) independent of the proton detector angle. These results agree with the prediction of a compound-nucleus theory. This suggests the existence of a strong compound-nuclear resonance in P^{29} at an excitation energy of 9.6 Mev. For lower proton beam energies, the symmetry direction, θ_0, shifts with a change in the proton detector angle or a change in the proton beam energy. These results are consistent with a direct-reaction mechanism.

*Now at Department of Physics, The University of Tennessee, Knoxville, Tennessee.

LOW-ENERGY p-p SCATTERING PHASE SHIFTS AND DISPERSION RELATIONS. Riazuddin, Department of Physics, Panjab University, Lahore, Pakistan (Received October 24, 1960).

Nucleon-nucleon dispersion relations have been used to discriminate between various sets of solutions given by MacGregor for low-energy proton-proton scattering. This has greatly reduced the ambiguity existing in the phase-shift analysis at low energy.

INVESTIGATION INTO THE ELASTIC SCATTERING OF $\Sigma^{\pm}$ HYPERONS ON HYDROGEN. F. Russell Stannard,* Lawrence Radiation Laboratory, University of California, Berkeley, California (Received October 20, 1960).

An investigation has been made into the elastic scattering of Σ hyperons on hydrogen. The experiment was based on a sample of 12 000 Σ particles formed in a propane bubble chamber by the interactions of 1.15-Bev/c K^- mesons. A total track length of 210 meters in the energy range 100 to 700 Mev has been examined.

Ten examples were found of the reaction $\Sigma^+ + p \rightarrow \Sigma^+ + p$, and six of the reaction $\Sigma^- + p \rightarrow \Sigma^- + p$. The estimates of the cross sections for the two processes are, respectively, 38^{+18}_{-14} mb and 10^{+6}_{-4} mb. The scattering-angle distributions in the c.m. system appear isotropic for the Σ^+ particles, and peaked forward for the Σ^- particles. The results are discussed in relation to various theoretical predictions, and, in particular, some evidence is found favoring the Gammel-Thaler method of treating the triplet odd-parity nucleon-nucleon potential.

*Present address: Physics Department, University College London, Gower Street, London W. C. 1, England.

CROSS SECTION AND DECAY ASYMMETRIES OF NEUTRAL V PARTICLES PRODUCED IN COPPER BY π^- MESONS. George R. Kalbfleisch, Lawrence Radiation Laboratory, University of California, Berkeley, California (Received August 17, 1960).

The charged mode of decay of 189 Λ and 77 K^0 particled produced by 1.12-Bev/c π^- mesons in the copper wall of the Berkeley 10-inch liquid hydrogen bubble chamber have been analyzed and their asymmetries calculated. The asymmetries have been examined for several interesting subgroups of the sample and for several directions of quantization. A fore-aft asymmetry in Λ decay has previously been reported in cosmic-ray interactions with complex nuclei and in some machine events of a similar nature. This asymmetry has recently been reviewed and summarized by Salmeron and Zichichi. They find a 3-standard-deviation effect, $\langle \alpha P_{\text{fore-aft}} \rangle_{\text{av}} = -0.56 \pm 0.15$. In contrast, the asymmetries found here for both Λ and K^0 are consistent with the assumption of the conservation of parity in the production process $\pi^- + p(\text{in nucleus}) \rightarrow \Lambda + K^0$.

The cross section for the associated production of ΛK^0 and $\Sigma^0 K^0$ has been determined as 10.5 ± 0.9 mb per copper nucleus. This value is somewhat larger than that expected on the assumption that the nucleons interact in first approximation as free nucleons possessing Fermi momentum according to an $A^{2/3}$ scaling of the hydrogen cross sections. This scaling predicts a value for this cross section of 7.4 ± 0.8 mb/nucleus.

Subsequent interactions of the hyperons with another nucleon in the same nucleus in which they were produced are frequent. A lower limit for the probability of scattering of the Λ can be set at 0.23 ± 0.07. This is in accordance with the observed $\Lambda + p$ cross sections.

HIGH-ENERGY NUCLEON-NUCLEON COLLISIONS. Freda Salzman and George Salzman, Department of Physics, University of Colorado, Boulder, Colorado (Received October 21, 1960).

The single virtual boson exchange interaction model is applied to high-energy inelastic nucleon-nucleon collisions over an energy range of several orders of magnitude. The phase space is discussed simply in terms of three "natural" phase-space variables, and a simple, exact formula is given for the "upper" boundary of these variables. The probability for a particular final-state configuration is then discussed in terms of the available phase space, the magnitude of the phase-space factor, and the magnitude of the average total "cross-section" factors that occur in this model. Qualitative features of experimental data for incident nucleon laboratory energies of 10, 10^2, and 10^3 Bev can be understood on the basis of this model.

Σ^0 - Λ^0 RELATIVE PARITY FROM Σ^0 DECAY. Louis Michel and Houchangue Rouhaninejad,* Laboratoire de Physique Théorique et Hautes Energies, Orsay, Seine et Oise, France (Received October 12, 1960).

In order to establish how ϵ, the Σ^0 - Λ^0 relative parity, can be measured from an actual bubble chamber experiment featuring polarized Σ^0 production and decay, followed by Λ^0 decay and γ-pair production or Dalitz pair in the Σ^0 decay, we constructed a correlation function depending on ϵ, another unknown parameter to be measured in the same experiment, and the energy and momenta of the different particles involved. Our study is Lorentz covariant, but the link with the usual "nonrelativistic" formalism is exhibited. In an Appendix it is shown that the polarization of Σ^0 produced in $\pi^- + p^+$ reactions is expected to be large.

*On leave of absence from the University of Teheran, Teheran, Iran.

USEFULNESS OF POLARIZED TARGETS AND THE POLARIZATION TRANSFER TENSOR IN RECONSTRUCTION OF THE NUCLEON-NUCLEON SCATTERING MATRIX. Clifford R. Schumacher and Hans A. Bethe, Laboratory of Nuclear Studies, Cornell University, Ithaca, New York (Received October 31, 1960).

A method is presented for completely removing the ambiguities arising in the reconstruction of the nucleon-nucleon scattering matrix from data at a given angle and energy due to the bilinear form of expressions for observable quantities. Our method utilizes only the amplitudes defined by Wolfenstein and Ashkin and is more direct and computationally simpler than the methods using unitarity and measurements at all angles or the phase-shift analyses; thus, it would provide an independent means of arriving at the correct set

of phase-shift solutions. Our method is based on a knowledge of the polarization transfer tensor $\mathcal{K}_{ik}$, which has a form complementary to the familiar polarization correlation tensor $\mathcal{C}_{ik}$. The $\mathcal{K}_{ik}$ tensor may be obtained from triple scattering experiments on the recoil nucleon similar to those used to determine the familiar depolarization tensor $\mathcal{D}_{ik}$, or from double scattering measurements on nucleons scattered from a polarized target.

It is also shown that the use of polarized targets would have many experimental advantages: They would permit (1) determination of the depolarization tensor $\mathcal{D}_{ik}$ for large scattering angles, without requiring the measurement of the polarization of a very slow nucleon, (2) determination of the correlation tensor $\mathcal{C}_{ik}$ by the measurement of the cross section for the scattering of a polarized beam by a polarized target, instead of the difficult simultaneous measurements of the polarizations of both the final nucleons, and (3) determination of the "difficult" components A' and R' of the $\mathcal{D}_{ik}$ and $\mathcal{K}_{ik}$ tensors by the measurement of the polarization of an initially unpolarized beam scattered by a polarized target.

REACTION $\bar{p}+p \rightarrow \bar{Y}+Y$. Janice Button, Philippe Eberhard, George R. Kalbfleisch, Joseph E. Lannutti,* Gerald R. Lynch, Bogdan C. Maglić, M. Lynn Stevenson, and Nguyen H. Xuong,† Lawrence Radiation Laboratory, University of California, Berkeley, California (Received October 24, 1960).

The study of the interaction $\bar{p}+p \rightarrow \bar{\Lambda}+\Lambda$, performed with the 72-inch hydrogen bubble chamber, has yielded 11 of these events in a total of 21 000 antiproton interactions at 1.61 Bev/c. The cross section for $\bar{\Lambda}+\Lambda$ production was estimated as 57 ± 19 μb. Nine of the 11 antilambdas went forward in the c.m. system. At the higher momentum of 1.99 Bev/c, one single-V and one double-V event fitting $\bar{\Lambda}+\Lambda$ production unambiguously and one single-V and one double-V event fitting $\bar{\Sigma}^0+\Lambda$ or $\Sigma^0+\bar{\Lambda}$ were observed in 4920 antiproton interactions. These events yield a $\bar{\Lambda}$-Λ production cross section of 55 ± 40 μb; this value is consistent with that predicted by the ratio of phase space on the basis of the 1.61-Bev/c data. No charged antisigma events were observed at the higher momentum. Three stages of particle separation utilizing velocity-selecting spectrometers were employed. At the lower momentum, background pions were one-third as numerous as antiprotons at the bubble chamber and the flux of antiprotons was about one per picture. At the higher momentum, the background pion to antiproton ratio was 1.8, and the flux of antiprotons was one every 13 pulses. Delta rays on incident interacting tracks were used to determine beam composition.

*Present address: Florida State University, Tallahassee, Florida.

†On leave from the Viet-Nam Atomic Energy Office, Viet-Nam, Indochina.

SPIN AND PARITY ANALYSIS FROM PRODUCTION AND DECAY OF HYPERON RESONANT STATES. R. Gatto* and H. P. Stapp, Physics Department and Lawrence Radiation Laboratory, University of California, Berkeley, California (Received November 1, 1960).

Processes dominated by the Λ-π resonance state, Y^*, should exhibit correlations permitting the determination of the Y^* spin; the relative parities of the Λ, Σ, K, and Y^*; and the ratios of the various hyperon-decay asymmetry parameters. The cases of Y^* spin $\frac{1}{2}$ and $\frac{3}{2}$ are examined in detail and a number of exact relations between measurable quantities are given for the various spin and parity assignments. The longitudinal component of polarization of the hyperon from the Y^* decay is, for parity-conserving reactions, the same for all final hyperons, independent of their parities. This allows the ratio of the decay asymmetry parameters for various hyperons to be determined. For a given Y^* spin the transverse hyperon polarization is determined by the longitudinal polarization up to a sign which is fixed by the Y^*-hyperon parity. Thus the transverse polarizations for final Λ and Σ particles will be the same or opposite if the parities are the same or opposite, respectively. For the spin $\frac{3}{2}$ case there are four independent contributions to the longitudinal polarization, each proportional to a different pseudoscalar spherical harmonic of the decay direction These give four independent experimental determinations of the ratios of the decay asymmetry parameters. Similarly, from the transverse components there are six independent determinations of relative parities.

If the initial and final states of the production process are restricted to S and P waves, all ten of the experimental parameters determining the

hyperon polarization are given, except for the aforementioned sign dependence on the Y^*-Y relative parity, by a single parameter in a manner fixed by the K-Y^* parity.

*Permanent address: Laboratori Nazionali, Frascati, Italy.

PROOF OF THE MANDELSTAM REPRESENTATION FOR EVERY ORDER IN PERTURBATION THEORY. Richard J. Eden, Clare College, Cambridge University, Cambridge, England (Received October 27, 1960).

It is proved that every term in the perturbation series for a scattering amplitude satisfies the Mandelstam representation when there are no anomalous thresholds. The absence of anomalous thresholds can be investigated from a few low-order diagrams, or reduced diagrams. Under certain conditions it is shown that their absence in fourth order ensures their absence in every order.

WAVE ZONE IN GENERAL RELATIVITY. R. Arnowitt, S. Deser, and C. W. Misner,* Syracuse University, Syracuse, New York, and Brandeis University, Waltham, Massachusetts (Received August 18, 1960).

It is shown that in general relativity a "wave zone" may be defined for systems which are asymptotically flat. In this region, gravitational radiation propagates freely, independent of its interior sources, and obeys the superposition principle. The independent dynamical variables of the full theory which describe the radiation are shown to be coordinate invariant in the wave zone and to satisfy the linearized theory's equations there. Thus, the basic properties of free waves in linear field theories (e.g., electrodynamics) are reproduced for the gravitational case. True waves are also clearly distinguished from so-called "coordinate waves." Reduction to asymptotic form (taking leading powers of $1/r$) is not identical to linearization, since, for example, the Newtonian-like $1/r$ part of the metric begins quadratically in the linear theory's variables. The Poynting vector of the full theory, which measures energy flux in the wave zone, is correspondingly shown to be given by the linearized theory's formula. This Poynting vector is also shown to be coordinate-invariant in the wave zone. All the physical quantities may therefore be evaluated in any frame becoming rectangular sufficiently rapidly. A brief discussion of measurements of the canonical variables in the wave zone is given. The relation between the present work and other treatments of gravitational radiation is examined.

*On leave from Palmer Physical Laboratory, Princeton University, Princeton, New Jersey.

RELATIVISTIC MODEL FIELD THEORY WITH FINITE SELF-MASSES. F. Zachariasen, California Institute of Technology, Pasadena, California (Received October 10, 1960).

A model field theory is invented in the following way: Dispersion relations in the energy are assumed to hold for all amplitudes. Unitarity gives the absorptive parts in the "physical" regions. If it is assumed that the absorptive parts are otherwise zero (in violation of crossing symmetry and the Mandelstam representation), then the dispersion relations and unitarity form an infinite set of coupled integral equations for all amplitudes. An exact solution (at least for the simplest amplitudes) to this set of equations can be found, in which all self-masses, etc., are finite. The solution is equivalent to summing a certain class of Feynman graphs, computed in the usual way. For a wide range of coupling constants, there are no "ghost" difficulties.

TWO-PION EXCHANGE MECHANISM IN K^+N SCATTERING. Benjamin W. Lee, Department of Physics, University of Pennsylvania, Philadelphia, Pennsylvania (Received October 31, 1960).

The exchange of two pions resonating in the $T=1$, $J=1$ state between the K^+ meson and nucleon in K^+N scattering is considered in the double dispersion representation to account for the energy dependence of the $J=\frac{1}{2}$ amplitudes. The result here is in qualitative agreement with that of Ferrari et al. obtained for K^-N scattering.